

Measurement-based entanglement purification for hybrid entangled state

Cheng-Chen Luo(罗程晨), Shi-Pu Gu(顾世浦), Xing-Fu Wang(王兴福), Lan Zhou(周澜), and Yu-Bo Sheng(盛宇波)

Citation: Chin. Phys. B, 2025, 34 (**3**): 030307. DOI: 10.1088/1674-1056/adb267
Journal homepage: http://cpb.iphy.ac.cn; http://iopscience.iop.org/cpb

What follows is a list of articles you may be interested in

Low-loss belief propagation decoder with Tanner graph in quantum error-correction codes

Dan-Dan Yan(颜丹丹), Xing-Kui Fan(范兴奎), Zhen-Yu Chen(陈祯羽), and Hong-Yang Ma(马鸿洋)
Chin. Phys. B, 2022, 31 (**1**): 010304. DOI: 10.1088/1674-1056/ac11cf

Direct measurement of the concurrence of hybrid entangled state based on parity check measurements

Man Zhang(张曼), Lan Zhou(周澜), Wei Zhong(钟伟), Yu-Bo Sheng(盛宇波)
Chin. Phys. B, 2019, 28 (**1**): 010301. DOI: 10.1088/1674-1056/28/1/010301

A novel scheme of hybrid entanglement swapping and teleportation using cavity QED in the small and large detuning regimes and quasi-Bell state measurement method

R Pakniat, M K Tavassoly, M H Zandi
Chin. Phys. B, 2016, 25 (**10**): 100303. DOI: 10.1088/1674-1056/25/10/100303

Hybrid entanglement concentration assisted with single coherent state

Rui Guo(郭锐), Lan Zhou(周澜), Shi-Pu Gu(顾世浦),Xing-Fu Wang(王兴福), Yu-Bo Sheng(盛宇波)
Chin. Phys. B, 2016, 25 (**3**): 030302. DOI: 10.1088/1674-1056/25/3/030302

Bidirectional quantum teleportation of unknown photons using path-polarization intra-particle hybrid entanglement and controlled-unitary gates via cross-Kerr nonlinearity

Jino Heo, Chang-Ho Hong, Jong-In Lim, Hyung-Jin Yang
Chin. Phys. B, 2015, 24 (**5**): 050304. DOI: 10.1088/1674-1056/24/5/050304

SPECIAL TOPIC — Quantum communication and quantum network

Measurement-based entanglement purification for hybrid entangled state

Cheng-Chen Luo(罗程晨)[1,3], Shi-Pu Gu(顾世浦)[2], Xing-Fu Wang(王兴福)[1], Lan Zhou(周澜)[1,†], and Yu-Bo Sheng(盛宇波)[2,3]

[1] *College of Science, Nanjing University of Posts and Telecommunications, Nanjing* 210023, *China*
[2] *College of Electronic and Optical Engineering & College of Flexible Electronics (Future Technology), Nanjing University of Posts and Telecommunications, Nanjing* 210023, *China*
[3] *Institute of Quantum Information and Technology, Nanjing University of Posts and Telecommunications, Nanjing* 210003, *China*

(Received 29 November 2024; revised manuscript received 11 January 2025; accepted manuscript online 5 February 2025)

Hybrid entangled states (HESs), which involve different particles with various degrees of freedom, have garnered significant attention and been applied in a wide range of quantum technologies. However, similar to other categories of entanglement, maximally HESs inevitably degrade to mixed states due to the environmental noise and operational imperfections. To address the degradation problem, measurement-based entanglement purification offers a feasible and robust solution alternative to conventional gate-based purification methods. In this paper, we propose a measurement-based hybrid entanglement purification protocol (MB-HEPP) for a certain kind of HES which consists of polarization photons and coherent states. We extend our methodology to several conditions, such as the multi-copy and multi-party scenarios, and the photon-loss condition. Compared with previous HEPPs, this protocol has several advantages. First, it does not depend on post-selection and the purified HESs can be retained for further application. Second, it does not require the Bell state measurement, but only uses the parity check with conventional linear optical elements, which makes it have the higher success probability and more feasible. Our MB-HEPP has potential applications in future heterogeneous quantum networks.

Keywords: hybrid entanglement, measurement-based entanglement purification, parity check

PACS: 03.67.Pp, 03.67.Hk, 03.65.Ud

DOI: 10.1088/1674-1056/adb267 **CSTR:** 32038.14.CPB.adb267

1. Introduction

As an essential property that distinguishes quantum physics from classical physics, quantum entanglement is central to various quantum communication and computation domains, including quantum teleportation,[1] quantum key distribution,[2] quantum secure direct communication,[3–6] quantum secret sharing,[7,8] quantum repeater,[9–11] distributed quantum computing[12] and other important branches of quantum technology.[13–19]

Hybrid entangled state (HES) represents a distinctive form of quantum entanglement involving various degrees of freedom (DOFs) across different particles. HES has garnered considerable interest due to its significant potential in various quantum domains.[11,20–26] Remarkably, the distinct structure of HES enables it to combine the strengths of different DOFs and mitigate the weaknesses inherent to each specific type of state.[27] Furthermore, HES serves as a crucial bridge to link practical physical systems with diverse natures, thereby facilitating the construction of heterogeneous quantum networks.[23,25] Among various types of HESs, the HES between discrete-variable (DV) and continuous-variable (CV) states has become particularly prominent, as it combines both the advantages of DV and CV encoding.[27] Such HES has been widely discussed in the generation,[20,28,29] quantum teleportation,[30] quantum repeaters,[11,31] quantum communication,[32–34] quantum computation[26,35] and some other important quantum tasks.[25,36,37]

Maximally entangled states are crucial resources for realizing the above quantum tasks. Unfortunately, maximally entangled states are susceptible to degradation due to the environmental noise and operational errors, which cause them to become mixed states. The degradation not only reduces the efficiency of protocols but also threatens their security. Entanglement purification is an effective method to distill some high-quality entanglement copies from a large number of low-quality entanglement copies through local operations and classical communications (LOCC).[38] In 1996, Bennett *et al.*[39] proposed the first entanglement purification protocol (EPP). Since then, numerous EPPs in both DV[39–44] and CV entanglement[45–49] have been proposed. The experiments of entanglement purification were realized in linear optics,[50,51] atoms,[52] electron-spin,[53] and superconductor systems.[54] In 2021, the first high-efficiency and long-distance entanglement purification experiment was realized and was first used

†Corresponding author. E-mail: zhoul@njupt.edu.cn

© 2025 Chinese Physical Society and IOP Publishing Ltd. All rights, including for text and data mining, AI training, and similar technologies, are reserved.

in the entanglement-based QKD to increase the key generation rate.[41] For HESs, the first hybrid entanglement purification protocol (HEPP) was proposed in 2013,[55] which specifically focused on the state $|\phi^+\rangle = \frac{1}{\sqrt{2}}(|H\rangle|\alpha\rangle + |V\rangle|-\alpha\rangle)$. Here, the single photon in $|H\rangle$ (horizontal polarization) or $|V\rangle$ (vertical polarization) belongs to the DV part, while the coherent states $|\pm\alpha\rangle$ with amplitudes $\pm\alpha$ belong to the CV part. Subsequently, the purification protocol for the HES with the photon-number state and the coherent state was proposed.[56] Recently, the hybrid logical qubit entanglement purification protocol was also proposed,[57] and some other recent HEPPs[58–60] in diverse systems.

The measurement-based entanglement purification protocol (MB-EPP)[49,61–65] is an important branch of EPP, serving as a key element in the measurement-based quantum repeater. Unlike conventional gate-based EPPs,[38] MB-EPP eliminates the need for complex quantum gates and instead harnesses the power of Bell state measurements (BSM) to drive the purification process. Therefore, MB-EPP reduces the technological requirement and makes MB-EPP more accessible for current experimental setups. Besides, MB-EPP provides a more robust solution against local noise and imperfections.[62]

In this work, we introduce an MB-HEPP for the hybrid entanglement involving polarization photons and coherent states. Unlike the previous MB-EPPs, we utilize the parity check instead of BSM to simplify the MB-HEPP and improve the success probability of the purification. We demonstrate that a single bit-flip error in either a CV qubit or a DV qubit can be purified. Furthermore, we extend our MB-HEPP to the multi-copy, multi-party cases, and consider the photon loss condition. Compared with previous HEPPs, this protocol has several advantages. First, it does not depend on post-selection and the purified HESs can be retained for further application. Second, it does not require the BSM, but only requires the parity check with conventional polarization beam splitter (PBS) and beam splitter (BS). In this way, our protocol has higher success probability and is more feasible.

The structure of this paper is as follows. In Section 2, we describe the principle of our MB-HEPP for the two-copy hybrid Bell states. In Section 3, we demonstrate the MB-HEPP for the multi-copy case. In Section 4, we extend this MB-HEPP for the multi-party HES. In Section 5, we address the error of photon loss with this MB-HEPP. Finally, the discussion and conclusion are presented in Section 6.

2. MB-HEPP for the two-copy hybrid Bell states

We begin by considering a simple example of a two-party HES, say, the hybrid Bell state. Assume the initial maximally entangled hybrid Bell state $|\phi^+\rangle$ generated from the source belongs to four Bell states of the form

$$\begin{aligned} |\phi^\pm\rangle &= \frac{1}{\sqrt{2}}(|H\rangle|\alpha\rangle \pm |V\rangle|-\alpha\rangle), \\ |\psi^\pm\rangle &= \frac{1}{\sqrt{2}}(|H\rangle|-\alpha\rangle \pm |V\rangle|\alpha\rangle). \end{aligned} \tag{1}$$

It is noteworthy that $|\langle-\alpha|\alpha\rangle|^2 = \mathrm{e}^{-4\alpha^2} \to 0$ for large α. Therefore, the coherent states can be regarded as approximately orthogonal.

Assume that the hybrid Bell state $|\phi^+\rangle$ is transmitted to Alice (a) and Bob (b) through quantum noisy channels, with the DV part sending to Alice and the CV part sending to Bob. Due to the environmental noise, the system may encounter errors. Here, we first consider a bit-flip error occurring in either the DV part or the CV part with the probability of $1-F$, which transforms the ideal state $|\phi^+\rangle_{\mathrm{ab}}$ into $|\psi^+\rangle_{\mathrm{ab}}$. Therefore, the entire system degrades to a mixed state as

$$\rho_{\mathrm{ab}} = F|\phi^+\rangle_{\mathrm{ab}}\langle\phi^+| + (1-F)|\psi^+\rangle_{\mathrm{ab}}\langle\psi^+|. \tag{2}$$

To perform this MB-HEPP, two identical copies of ρ_{ab} are required, denoted as ρ_{a1b1} and ρ_{a2b2}. Thus, the entire initial system can be expressed as $\rho_{\mathrm{a1b1}} \otimes \rho_{\mathrm{a2b2}}$, representing a probabilistic mixture of four hybrid pure states. In detail, with a probability of F^2, the system is in the state of $|\phi^+\rangle_{\mathrm{a1b1}} \otimes |\phi^+\rangle_{\mathrm{a2b2}}$. With a probability of $(1-F)^2$, the system is in the state of $|\psi^+\rangle_{\mathrm{a1b1}} \otimes |\psi^+\rangle_{\mathrm{a2b2}}$. With equal probability of $F(1-F)$, the system is in the state of $|\phi^+\rangle_{\mathrm{a1b1}} \otimes |\psi^+\rangle_{\mathrm{a2b2}}$ or $|\psi^+\rangle_{\mathrm{a1b1}} \otimes |\phi^+\rangle_{\mathrm{a2b2}}$.

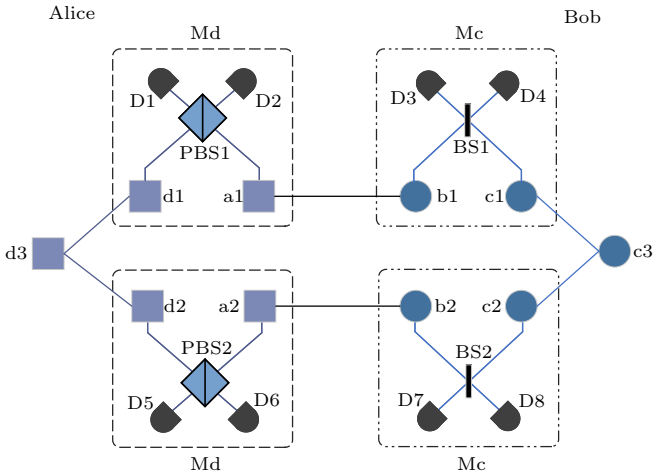


Fig. 1. Schematic diagram of the measurement-based purification protocol for the two-copy hybrid Bell states. Two identical pairs of mixed hybrid Bell states in a1b1 and a2b2 modes are shared by Alice and Bob. Alice receives the DV part, and Bob receives the CV part. The setups labeled as Md and Mc are used to perform the parity checks on the DV and CV parts, respectively. Two pairs of resource states entangled in modes d1d2d3 and c1c2c3 are required.

Figure 1 illustrates the schematic principle of our MB-HEPP. Alice and Bob should prepare two pairs of resource states in d1d2d3 and c1c2c3 modes, respectively. In this two-copy protocol, the resource states at Alice's and Bob's sides

are the DV and CV Greenberger–Horne–Zeilinger (GHZ) states, respectively, which have the forms of

$$\begin{aligned}|\mathrm{GHZ_D}\rangle_{\mathrm{d1d2d3}} &= \frac{1}{\sqrt{2}}(|HHH\rangle+|VVV\rangle)_{\mathrm{d1d2d3}},\\ |\mathrm{GHZ_C}\rangle_{\mathrm{c1c2c3}} &= \frac{1}{N_3}(|\alpha,\alpha,\alpha\rangle+|-\alpha,-\alpha,-\alpha\rangle)_{\mathrm{c1c2c3}}. \quad (3)\end{aligned}$$

Here $N_3=\sqrt{2+2\mathrm{e}^{-6\alpha^2}}$ is the normalization parameter. Consequently, the two hybrid mixed states combined with two resource states are represented as $\rho_{\mathrm{a1b1}}\otimes\rho_{\mathrm{a2b2}}\otimes|\mathrm{GHZ_D}\rangle_{\mathrm{d1d2d3}}\otimes|\mathrm{GHZ_C}\rangle_{\mathrm{c1c2c3}}$.

Alice and Bob perform the parity checks on the photons in a*i*d*i* and b*i*c*i* ($i=1,2$), respectively. In detail, for the DV part at Alice's side, the parity check setup denoted as Md consists of a BS and two photon detectors. For the CV part at Bob's side, the parity check setup labeled as Mc includes a PBS and two photon detectors. BS can transform $|\alpha\rangle_{\mathrm{a1}}|\beta\rangle_{\mathrm{d1}}\rightarrow|\frac{\alpha+\beta}{\sqrt{2}}\rangle_{\mathrm{a1}}|\frac{\alpha-\beta}{\sqrt{2}}\rangle_{\mathrm{d1}}$,[55] while PBS can completely transmit the photon in $|H\rangle$ and entirely reflect the photon in $|V\rangle$. The photon detectors can merely distinguish the presence or absence of photons, but cannot distinguish the photon number. Specifically, in the Md, after passing through the PBS, the four polarization states evolve to

$$\begin{aligned}|H\rangle|H\rangle_{\mathrm{a1d1}} &\xrightarrow{\mathrm{Md}} |H\rangle_{\mathrm{a1}}|H\rangle_{\mathrm{d1}}\rightarrow|0^{\mathrm{d}}\rangle,\\ |V\rangle|V\rangle_{\mathrm{a1d1}} &\xrightarrow{\mathrm{Md}} |V\rangle_{\mathrm{d1}}|V\rangle_{\mathrm{a1}}\rightarrow|0^{\mathrm{d}}\rangle,\\ |H\rangle|V\rangle_{\mathrm{a1d1}} &\xrightarrow{\mathrm{Md}} |H\rangle_{\mathrm{a1}}|V\rangle_{\mathrm{a1}}\rightarrow|1^{\mathrm{d}}\rangle,\\ |V\rangle|H\rangle_{\mathrm{a1d1}} &\xrightarrow{\mathrm{Md}} |V\rangle_{\mathrm{d1}}|H\rangle_{\mathrm{d1}}\rightarrow|1^{\mathrm{d}}\rangle. \quad (4)\end{aligned}$$

It is clear that the polarization even-parity states $|H\rangle|H\rangle$ and $|V\rangle|V\rangle$ will lead both detectors D1 and D2 to click, while the odd-parity states $|H\rangle|V\rangle$ and $|V\rangle|H\rangle$ will only lead a click on D1 or D2. The even and odd of DV parity check results are denoted as $|0^{\mathrm{d}}\rangle$ and $|1^{\mathrm{d}}\rangle$. Therefore, by counting the clicks of the photon detectors, one can distinguish the polarization parity of the input state. On the other hand, in Mc at Bob's side, after passing through BS, the four coherent states evolve to[55]

$$\begin{aligned}|\alpha\rangle|\alpha\rangle_{\mathrm{b1c1}} &\xrightarrow{\mathrm{Mc}} |\sqrt{2}\alpha\rangle_{\mathrm{b1}}|0\rangle_{\mathrm{c1}}\rightarrow|0^{\mathrm{c}}\rangle,\\ |-\alpha\rangle|-\alpha\rangle_{\mathrm{b1c1}} &\xrightarrow{\mathrm{Mc}} |-\sqrt{2}\alpha\rangle_{\mathrm{b1}}|0\rangle_{\mathrm{c1}}\rightarrow|0^{\mathrm{c}}\rangle,\\ |\alpha\rangle|-\alpha\rangle_{\mathrm{b1c1}} &\xrightarrow{\mathrm{Mc}} |0\rangle_{\mathrm{b1}}|\sqrt{2}\alpha\rangle_{\mathrm{c1}}\rightarrow|1^{\mathrm{c}}\rangle,\\ |-\alpha\rangle|\alpha\rangle_{\mathrm{b1c1}} &\xrightarrow{\mathrm{Mc}} |0\rangle_{\mathrm{b1}}|-\sqrt{2}\alpha\rangle_{\mathrm{c1}}\rightarrow|1^{\mathrm{c}}\rangle. \quad (5)\end{aligned}$$

Similarly, the CV even-parity states $|\alpha\rangle|\alpha\rangle$ and $|-\alpha\rangle|-\alpha\rangle$ will cause a click of the detector D4, while the odd-parity states $|\alpha\rangle|-\alpha\rangle$ and $|-\alpha\rangle|\alpha\rangle$ will cause a click of the detector D3. The even and odd of CV parity check results are denoted as $|0^{\mathrm{c}}\rangle$ and $|1^{\mathrm{c}}\rangle$, respectively. Thus, one can distinguish the CV parity of the input state by observing which photon detector registers a click.

Successful purification occurs when Alice and Bob obtain eight kinds of "proper cases". For example, with the probability of F^2, the state $\rho_{\mathrm{a1b1}}\otimes\rho_{\mathrm{a2b2}}\otimes|\mathrm{GHZ_D}\rangle_{\mathrm{d1d2d3}}\otimes|\mathrm{GHZ_C}\rangle_{\mathrm{c1c2c3}}$ can be written as

$$\begin{aligned}&|\phi^+\rangle_{\mathrm{a1b1}}|\phi^+\rangle_{\mathrm{a2b2}}|\mathrm{GHZ_D}\rangle_{\mathrm{d1d2d3}}|\mathrm{GHZ_C}\rangle_{\mathrm{c1c2c3}}\\ =&\ \frac{1}{\sqrt{2}}(|H\rangle|\alpha\rangle+|V\rangle|-\alpha\rangle)_{\mathrm{a1b1}}\\ &\otimes\frac{1}{\sqrt{2}}(|H\rangle|\alpha\rangle+|V\rangle|-\alpha\rangle)_{\mathrm{a2b2}}\\ &\otimes\frac{1}{\sqrt{2}}(|HHH\rangle+|VVV\rangle)_{\mathrm{d1d2d3}}\\ &\otimes\frac{1}{N_3}(|\alpha,\alpha,\alpha\rangle+|-\alpha,-\alpha,-\alpha\rangle)_{\mathrm{c1c2c3}}. \quad (6)\end{aligned}$$

Then, by selecting the cases where the Md result of each hybrid pair has the same parity as the Mc result, say, $|0^{\mathrm{d}}0^{\mathrm{d}}0^{\mathrm{c}}0^{\mathrm{c}}\rangle$, $|0^{\mathrm{d}}1^{\mathrm{d}}0^{\mathrm{c}}1^{\mathrm{c}}\rangle$, $|1^{\mathrm{d}}0^{\mathrm{d}}1^{\mathrm{c}}0^{\mathrm{c}}\rangle$ or $|1^{\mathrm{d}}1^{\mathrm{d}}1^{\mathrm{c}}1^{\mathrm{c}}\rangle$ (the details are shown in Appendix A), the quantum state of the photons in d3c3 modes transforms to

$$|\phi^+\rangle_{\mathrm{d3c3}}=\frac{1}{\sqrt{2}}(|H\rangle|\alpha\rangle+|V\rangle|-\alpha\rangle)_{\mathrm{d3c3}}. \quad (7)$$

Alternatively, by selecting the cases where the Md result and Mc result for each hybrid pair are different, say, $|0^{\mathrm{d}}0^{\mathrm{d}}1^{\mathrm{c}}1^{\mathrm{c}}\rangle$, $|0^{\mathrm{d}}1^{\mathrm{d}}1^{\mathrm{c}}0^{\mathrm{c}}\rangle$, $|1^{\mathrm{d}}0^{\mathrm{d}}0^{\mathrm{c}}1^{\mathrm{c}}\rangle$ and $|1^{\mathrm{d}}1^{\mathrm{d}}0^{\mathrm{c}}0^{\mathrm{c}}\rangle$, the quantum state of the photons in mode d3c3 is $|\psi^+\rangle_{\mathrm{d3c3}}=\frac{1}{\sqrt{2}}(|H\rangle|-\alpha\rangle+|V\rangle|\alpha\rangle)_{\mathrm{d3c3}}$. In this scenario, the parties can perform a bit-flip operation on the single photon or the coherent state to obtain the desired state $|\phi^+\rangle_{\mathrm{d3c3}}$. Therefore, the above eight parity measurement results are the "proper cases", which lead to the success of the hybrid entanglement purification.

Similarly, the whole quantum system is in the state $|\psi^+\rangle_{\mathrm{a1b1}}|\psi^+\rangle_{\mathrm{a2b2}}\ |\mathrm{GHZ_D}\rangle_{\mathrm{d1d2d3}}|\mathrm{GHZ_C}\rangle_{\mathrm{c1c2c3}}$ with the probability of $(1-F)^2$. After Alice and Bob performing the DV and CV parity checks and selecting the four "proper cases" $|0^{\mathrm{d}}0^{\mathrm{d}}0^{\mathrm{c}}0^{\mathrm{c}}\rangle$, $|0^{\mathrm{d}}1^{\mathrm{d}}0^{\mathrm{c}}1^{\mathrm{c}}\rangle$, $|1^{\mathrm{d}}0^{\mathrm{d}}1^{\mathrm{c}}0^{\mathrm{c}}\rangle$ and $|1^{\mathrm{d}}1^{\mathrm{d}}1^{\mathrm{c}}1^{\mathrm{c}}\rangle$, the whole system evolves to

$$|\psi^+\rangle_{\mathrm{d3c3}}=\frac{1}{\sqrt{2}}(|H\rangle|-\alpha\rangle+|V\rangle|\alpha\rangle)_{\mathrm{d3c3}}. \quad (8)$$

Additionally, the whole system collapses to $|\phi^+\rangle_{\mathrm{d3c3}}=\frac{1}{\sqrt{2}}(|H\rangle|\alpha\rangle+|V\rangle|-\alpha\rangle)_{\mathrm{d3c3}}$ if the parity check result is one of the other four "proper cases" $|0^{\mathrm{d}}0^{\mathrm{d}}1^{\mathrm{c}}1^{\mathrm{c}}\rangle$, $|0^{\mathrm{d}}1^{\mathrm{d}}1^{\mathrm{c}}0^{\mathrm{c}}\rangle$, $|1^{\mathrm{d}}0^{\mathrm{d}}0^{\mathrm{c}}1^{\mathrm{c}}\rangle$ and $|1^{\mathrm{d}}1^{\mathrm{d}}0^{\mathrm{c}}0^{\mathrm{c}}\rangle$. It can be transformed to $|\psi^+\rangle_{\mathrm{d3c3}}$ through a bit-flip operation performed by Alice or Bob.

On the other hand, the crossed combinations $|\phi^+\rangle_{\mathrm{a1b1}}|\psi^+\rangle_{\mathrm{a2b2}}$ and $|\psi^+\rangle_{\mathrm{a1b1}}|\phi^+\rangle_{\mathrm{a2b2}}$ of $\rho_{\mathrm{a1b1}}\otimes\rho_{\mathrm{a2b2}}$ combined with $|\mathrm{GHZ_D}\rangle_{\mathrm{d1d2d3}}\ |\mathrm{GHZ_C}\rangle_{\mathrm{c1c2c3}}$ can be automatically eliminated, for they could only lead to eight different parity check results $|0^{\mathrm{d}}0^{\mathrm{d}}0^{\mathrm{c}}1^{\mathrm{c}}\rangle$, $|0^{\mathrm{d}}1^{\mathrm{d}}0^{\mathrm{c}}0^{\mathrm{c}}\rangle$, $|1^{\mathrm{d}}0^{\mathrm{d}}1^{\mathrm{c}}1^{\mathrm{c}}\rangle$, $|1^{\mathrm{d}}1^{\mathrm{d}}1^{\mathrm{c}}0^{\mathrm{c}}\rangle$, $|0^{\mathrm{d}}0^{\mathrm{d}}1^{\mathrm{c}}0^{\mathrm{c}}\rangle$, $|0^{\mathrm{d}}1^{\mathrm{d}}1^{\mathrm{c}}1^{\mathrm{c}}\rangle$, $|1^{\mathrm{d}}0^{\mathrm{d}}0^{\mathrm{c}}0^{\mathrm{c}}\rangle$ and $|1^{\mathrm{d}}1^{\mathrm{d}}0^{\mathrm{c}}1^{\mathrm{c}}\rangle$, which have odd number of 0 and 1. These eight parity check results lead to a failure of this MB-HEPP. Thus, by selecting the eight

kinds of "proper cases", the whole system in d3c3 transforms to a new hybrid mixed state as

$$\rho_{\mathrm{d3c3}} = F_1|\phi^+\rangle_{\mathrm{d3c3}}\langle\phi^+| + (1-F_1)|\psi^+\rangle_{\mathrm{d3c3}}\langle\psi^+|, \quad (9)$$

where the fidelity F_1 of the target state $|\phi^+\rangle_{\mathrm{d3c3}}$ can be expressed as

$$F_1 = \frac{F^2}{F^2+(1-F)^2}. \quad (10)$$

The success probability is $P_1 = F^2+(1-F)^2$. If the initial fidelity $F > 1/2$, the purification process will yield $F_1 > F$. Furthermore, if a phase-flip error occurs instead of a bit-flip error in $|\phi^+\rangle_{\mathrm{ab}}$, the phase-flip error can be converted into a bit-flip error through the Hadamard operations[55] and then purified using the above purification protocol in the next round.

3. MB-HEPP for the multi-copy hybrid Bell states

In this section, we discuss our MB-HEPP employing multi-copy hybrid Bell states. As illustrated in Fig. 2, N copies of identical hybrid mixed states ρ_{a1b1}, ρ_{a2b2}, …, ρ_{aNbN} , with the form of Eq. (2) are needed in each iteration. The resource states for the DV and CV parts can be given by

$$|\mathrm{GHZ}_{\mathrm{D}n}\rangle = \frac{1}{\sqrt{2}}(|HH\cdots H\rangle + |VV\cdots V\rangle)_{\mathrm{d1d2}\cdots\mathrm{d}n}, \quad (11)$$

$$|\mathrm{GHZ}_{\mathrm{C}n}\rangle = \frac{1}{N_n}(|\alpha,\alpha,\ldots,\alpha\rangle + |-\alpha,-\alpha,\ldots,-\alpha\rangle)_{\mathrm{c1c2}\cdots\mathrm{c}n}. \quad (12)$$

Here $n = N+1$, $N_n = \sqrt{2\pm 2\mathrm{e}^{-2(N+1)\alpha^2}}$ is the normalization parameter.

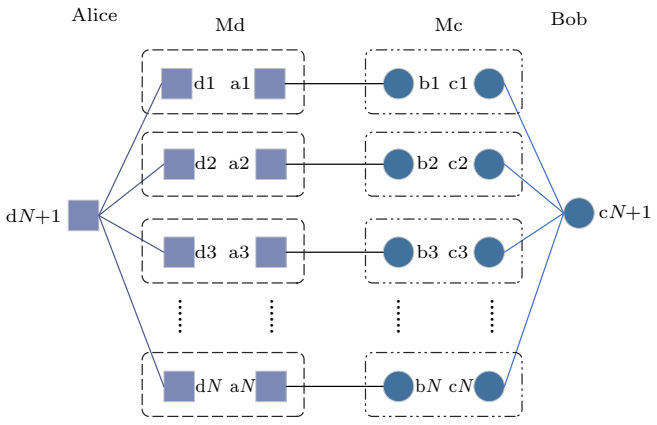


Fig. 2. A schematic diagram of the MB-HEPP for multi-copy hybrid Bell states. Multiple identical pairs of mixed hybrid Bell states are shared by Alice and Bob. Alice receives the DV parts, and Bob receives the CV parts. Alice and Bob are required to prepare the DV GHZ state and CV GHZ state, respectively.

For simplicity, we illustrate the purification principle in the case of $N = 3$. In this case, three copies of identical hybrid states $|\phi^+\rangle_{\mathrm{a1b1}}$, $|\phi^+\rangle_{\mathrm{a2b2}}$ and $|\phi^+\rangle_{\mathrm{a3b3}}$ are distributed to Alice and Bob. The resource states are written as

$$\begin{aligned}|\mathrm{GHZ}_{\mathrm{D4}}\rangle &= \frac{1}{\sqrt{2}}(|HHHH\rangle + |VVVV\rangle)_{\mathrm{d1d2d3d4}},\\ |\mathrm{GHZ}_{\mathrm{C4}}\rangle &= \frac{1}{N_4}(|\alpha,\alpha,\alpha,\alpha\rangle\\ &\quad + |-\alpha,-\alpha,-\alpha,-\alpha\rangle)_{\mathrm{c1c2c3c4}},\end{aligned} \quad (13)$$

where $N_4 = \sqrt{2\pm 2\mathrm{e}^{-8\alpha^2}}$. If a bit-flip error occurs with the probability of $1-F$, the entire three-copy hybrid system is represented by $\rho_{\mathrm{a1b1}}\otimes\rho_{\mathrm{a2b2}}\otimes\rho_{\mathrm{a3b3}}$, comprising of eight pure states. In detail, with a probability of F^3, the system is in the state of $|\phi^+\rangle_{\mathrm{a1b1}}\otimes|\phi^+\rangle_{\mathrm{a2b2}}\otimes|\phi^+\rangle_{\mathrm{a3b3}}$. With a probability of $(1-F)^3$, the system is in the state of $|\psi^+\rangle_{\mathrm{a1b1}}\otimes|\psi^+\rangle_{\mathrm{a2b2}}\otimes|\psi^+\rangle_{\mathrm{a3b3}}$. With an equal probability of $F^2(1-F)$, the system may be $|\phi^+\rangle_{\mathrm{a1b1}}\otimes|\phi^+\rangle_{\mathrm{a2b2}}\otimes|\psi^+\rangle_{\mathrm{a3b3}}$, $|\phi^+\rangle_{\mathrm{a1b1}}\otimes|\psi^+\rangle_{\mathrm{a2b2}}\otimes|\phi^+\rangle_{\mathrm{a3b3}}$, or $|\psi^+\rangle_{\mathrm{a1b1}}\otimes|\phi^+\rangle_{\mathrm{a2b2}}\otimes|\phi^+\rangle_{\mathrm{a3b3}}$. With an equal probability of $F(1-F)^2$, the system may be in $|\psi^+\rangle_{\mathrm{a1b1}}\otimes|\psi^+\rangle_{\mathrm{a2b2}}\otimes|\phi^+\rangle_{\mathrm{a3b3}}$, $|\phi^+\rangle_{\mathrm{a1b1}}\otimes|\psi^+\rangle_{\mathrm{a2b2}}|\psi^+\rangle_{\mathrm{a3b3}}$, or $|\psi^+\rangle_{\mathrm{a1b1}}\otimes|\phi^+\rangle_{\mathrm{a2b2}}\otimes|\psi^+\rangle_{\mathrm{a3b3}}$.

Hence, these three copies of hybrid mixed states combined with two resource states can be written as $\rho_{\mathrm{a1b1}}\otimes\rho_{\mathrm{a2b2}}\otimes\rho_{\mathrm{a3b3}}\otimes|\mathrm{GHZ}_{\mathrm{D4}}\rangle_{\mathrm{d1d2d3d4}}\otimes|\mathrm{GHZ}_{\mathrm{C4}}\rangle_{\mathrm{c1c2c3c4}}$. The purification principle follows the similar procedure to that of the two-copy case. After Alice and Bob each performing three parity checks, they select the "proper cases". For example, with the probability of F^3, the whole quantum state is

$$\begin{aligned}&|\phi^+\rangle_{\mathrm{a1b1}}|\phi^+\rangle_{\mathrm{a2b2}}|\phi^+\rangle_{\mathrm{a3b3}}|\mathrm{GHZ}_{\mathrm{D4}}\rangle_{\mathrm{d1d2d3d4}}|\mathrm{GHZ}_{\mathrm{C4}}\rangle_{\mathrm{c1c2c3c4}}\\ &= \frac{1}{\sqrt{2}}(|H\rangle|\alpha\rangle + |V\rangle|-\alpha\rangle)_{\mathrm{a1b1}}\\ &\quad\otimes\frac{1}{\sqrt{2}}(|H\rangle|\alpha\rangle + |V\rangle|-\alpha\rangle)_{\mathrm{a2b2}}\\ &\quad\otimes\frac{1}{\sqrt{2}}(|H\rangle|\alpha\rangle + |V\rangle|-\alpha\rangle)_{\mathrm{a3b3}}\\ &\quad\otimes\frac{1}{\sqrt{2}}(|HHHH\rangle + |VVVV\rangle)_{\mathrm{d1d2d3d4}}\\ &\quad\otimes\frac{1}{N_4}(|\alpha,\alpha,\alpha,\alpha\rangle + |-\alpha,-\alpha,-\alpha,-\alpha\rangle)_{\mathrm{c1c2c3c4}}.\end{aligned} \quad (14)$$

Therefore, by selecting the eight "proper cases" as

$$\begin{aligned}&|0^{\mathrm{d}}0^{\mathrm{d}}0^{\mathrm{d}}0^{\mathrm{c}}0^{\mathrm{c}}0^{\mathrm{c}}\rangle, \quad |0^{\mathrm{d}}0^{\mathrm{d}}1^{\mathrm{d}}0^{\mathrm{c}}0^{\mathrm{c}}1^{\mathrm{c}}\rangle,\\ &|0^{\mathrm{d}}1^{\mathrm{d}}0^{\mathrm{d}}0^{\mathrm{c}}1^{\mathrm{c}}0^{\mathrm{c}}\rangle, \quad |1^{\mathrm{d}}0^{\mathrm{d}}0^{\mathrm{d}}1^{\mathrm{c}}0^{\mathrm{c}}0^{\mathrm{c}}\rangle,\\ &|0^{\mathrm{d}}1^{\mathrm{d}}1^{\mathrm{d}}0^{\mathrm{c}}1^{\mathrm{c}}1^{\mathrm{c}}\rangle, \quad |1^{\mathrm{d}}0^{\mathrm{d}}1^{\mathrm{d}}1^{\mathrm{c}}0^{\mathrm{c}}1^{\mathrm{c}}\rangle,\\ &|1^{\mathrm{d}}1^{\mathrm{d}}0^{\mathrm{d}}1^{\mathrm{c}}1^{\mathrm{c}}0^{\mathrm{c}}\rangle, \quad |1^{\mathrm{d}}1^{\mathrm{d}}1^{\mathrm{d}}1^{\mathrm{c}}1^{\mathrm{c}}1^{\mathrm{c}}\rangle,\end{aligned}$$

from the items in

$$\begin{aligned}&|\phi^+\rangle_{\mathrm{a1b1}}|\phi^+\rangle_{\mathrm{a2b2}}|\phi^+\rangle_{\mathrm{a3b3}}(|HHHH\rangle|\alpha,\alpha,\alpha,\alpha\rangle\\ &+|VVVV\rangle|-\alpha,-\alpha,-\alpha,-\alpha\rangle)_{\mathrm{d1d2d3d4c1c2c3c4}},\end{aligned}$$

the parties can obtain the state

$$|\phi^+\rangle_{\mathrm{d4c4}} = \frac{1}{\sqrt{2}}(|H\rangle|\alpha\rangle + |V\rangle|-\alpha\rangle)_{\mathrm{d4c4}}. \quad (15)$$

Alternatively, the parties can select the other eight "proper cases" as

$$|0^{\rm d}0^{\rm d}0^{\rm d}1^{\rm c}1^{\rm c}1^{\rm c}\rangle,\quad |0^{\rm d}0^{\rm d}1^{\rm d}1^{\rm c}1^{\rm c}0^{\rm c}\rangle,$$
$$|0^{\rm d}1^{\rm d}0^{\rm d}1^{\rm c}0^{\rm c}1^{\rm c}\rangle,\quad |1^{\rm d}0^{\rm d}0^{\rm d}0^{\rm c}1^{\rm c}1^{\rm c}\rangle,$$
$$|1^{\rm d}1^{\rm d}0^{\rm d}0^{\rm c}0^{\rm c}1^{\rm c}\rangle,\quad |1^{\rm d}0^{\rm d}1^{\rm d}0^{\rm c}1^{\rm c}0^{\rm c}\rangle,$$
$$|0^{\rm d}1^{\rm d}1^{\rm d}1^{\rm c}0^{\rm c}0^{\rm c}\rangle,\quad |1^{\rm d}1^{\rm d}1^{\rm d}0^{\rm c}0^{\rm c}0^{\rm c}\rangle,$$

from the items in

$$|\phi^+\rangle_{\rm a1b1}|\phi^+\rangle_{\rm a2b2}|\phi^+\rangle_{\rm a3b3}(|HHHH\rangle|-\alpha,-\alpha,-\alpha,-\alpha\rangle$$
$$+|VVVV\rangle|\alpha,\alpha,\alpha,\alpha\rangle)_{\rm d1d2d3d4c1c2c3c4}.$$

Then, they can obtain the state $|\psi^+\rangle_{\rm d4c4}=\frac{1}{\sqrt{2}}(|H\rangle|-\alpha\rangle+|V\rangle|\alpha\rangle)_{\rm d4c4}$, which can be transformed to $|\phi^+\rangle_{\rm d4c4}$ with the bit-flip operation performed by Alice or Bob.

Conversely, by selecting the above sixteen "proper cases" and performing an appropriate operation, the state $|\psi^+\rangle_{\rm a1b1}|\psi^+\rangle_{\rm a2b2}|\psi^+\rangle_{\rm a3b3}|{\rm GHZ_{D4}}\rangle_{\rm d1d2d3d4}|{\rm GHZ_{C4}}\rangle_{\rm c1c2c3c4}$ collapses to

$$|\psi^+\rangle_{\rm d4c4}=\frac{1}{\sqrt{2}}(|H\rangle|-\alpha\rangle+|V\rangle|\alpha\rangle)_{\rm d4c4}. \tag{16}$$

On the other hand, the other six cross items of the whole hybrid system $\rho_{\rm a1b1}\otimes\rho_{\rm a2b2}\otimes\rho_{\rm a3b3}$ will never lead to any of the above sixteen "proper cases". Therefore, they can be eliminated automatically according to the selection principle. Finally, Alice and Bob can obtain a new hybrid mixed state as

$$\rho_{\rm d4c4}=F_2|\phi^+\rangle_{\rm d4c4}\langle\phi^+|+(1-F_2)|\psi^+\rangle_{\rm d4c4}\langle\psi^+|, \tag{17}$$

with the success probability $P_2=F^3+(1-F)^3$. Here, the fidelity F_2 can be calculated as

$$F_2=\frac{F^3}{F^3+(1-F)^3}. \tag{18}$$

Moreover, we can extend this MB-HEPP to the N-copy case. After performing this MB-HEPP on an N-copy system, one obtains the new hybrid mixed state as

$$\rho_{{\rm d}N+1,{\rm c}N+1}=F_N|\phi^+\rangle_{{\rm d}N+1,{\rm c}N+1}\langle\phi^+|$$
$$+(1-F_N)|\psi^+\rangle_{{\rm d}N+1,{\rm c}N+1}\langle\psi^+|, \tag{19}$$

where the fidelity F_N can be calculated as

$$F_N=\frac{F^N}{F^N+(1-F)^N}. \tag{20}$$

The success probability can be calculated as $P_{2N}=F^N+(1-F)^N$. If the initial fidelity $F>1/2$, they can achieve the resultant fidelity $F_N>F$. Moreover, F_N increases with the growth of N. It indicates that by consuming more low-quality HESs, the parties can obtain a higher fidelity.

4. MB-HEPP for the multi-party hybrid entanglement

In the section, we can extend this MB-HEPP to the purification of the multi-party HES. In this section, we consider that the target hybrid state $|\phi^{\pm}_{M,N}\rangle$ is distributed to $M+N$ parties in the form of

$$|\phi^{\pm}_{M,N}\rangle=\frac{1}{\sqrt{2}}(|HH\cdots H\rangle_M|\alpha,\alpha,\ldots,\alpha\rangle_N$$
$$\pm|VV\cdots V\rangle_M|-\alpha,-\alpha,\ldots,-\alpha\rangle_N), \tag{21}$$

where the DV part is sent to M parties and the CV part is sent to N parties, respectively. After the photons transmitting through noisy quantum channels, the bit-flip error may occur. If a bit-flip error occurs in the CV part, the initial state becomes

$$|\psi^{\rm c\pm}_{M,N}\rangle=\frac{1}{\sqrt{2}}(|HH\cdots H\rangle_M|\alpha,\alpha,\ldots,-\alpha\rangle_N$$
$$\pm|VV\cdots V\rangle_M|-\alpha,-\alpha,\ldots,\alpha\rangle_N). \tag{22}$$

On the other hand, if a bit-flip error occurs in the DV part, the initial state becomes

$$|\psi^{\rm d\pm}_{M,N}\rangle=\frac{1}{\sqrt{2}}(|HH\cdots V\rangle_M|\alpha,\alpha,\ldots,\alpha\rangle_N$$
$$\pm|VV\cdots H\rangle_M|-\alpha,-\alpha,\ldots,-\alpha\rangle_N). \tag{23}$$

Now we explain the purification process for the multi-party HES. The schematic principle of the multi-party MB-HEPP is shown in Fig. 3. For simplicity, we take the case of $M=N=2$ for example to demonstrate the purification principle. Suppose that the DV part is distributed to Alice and Bob, while the CV part is distributed to Charlie and David. In this case, the initial hybrid state can be written as

$$|\phi^+_{2,2}\rangle_{\rm abcd}=\frac{1}{\sqrt{2}}(|H,H,\alpha,\alpha\rangle_{\rm abcd}+|V,V,-\alpha,-\alpha\rangle_{\rm abcd}). \tag{24}$$

We first consider a bit-flip error occurring in the CV part with the probability of $1-F_{\rm c}$, which transforms $|\phi^+_{2,2}\rangle_{\rm abcd}$ to $|\psi^{\rm c+}_{2,2}\rangle_{\rm abcd}$ as

$$|\psi^{\rm c+}_{2,2}\rangle_{\rm abcd}=\frac{1}{\sqrt{2}}(|H,H,\alpha,-\alpha\rangle_{\rm abcd}+|V,V,-\alpha,\alpha\rangle_{\rm abcd}). \tag{25}$$

Therefore, the hybrid system degrades to a mixed state with the form of

$$\rho^{\rm c}_{\rm abcd}=F_{\rm c}|\phi^+_{2,2}\rangle_{\rm abcd}\langle\phi^+_{2,2}|+(1-F_{\rm c})|\psi^{\rm c+}_{2,2}\rangle_{\rm abcd}\langle\psi^{\rm c+}_{2,2}|. \tag{26}$$

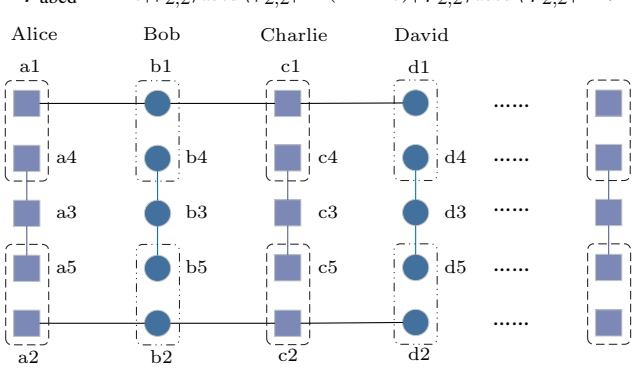


Fig. 3. Schematic diagram of the MB-HEPP for the multi-party HES. Two identical copies of mixed hybrid states are shared by multiple parties.

In order to perform this MB-HEPP, we still require two identical copies of hybrid entanglement, denoted as $\rho^{c}_{a1b1c1d1}$ and $\rho^{c}_{a2b2c2d2}$. Hence, the initial system $\rho^{c}_{a1b1c1d1}\otimes\rho^{c}_{a2b2c2d2}$ represents a probabilistic mixture of four hybrid pure states. In detail, with a probability of F_c^2, the system is in the state of $|\phi^+_{2,2}\rangle_{a1b1c1d1}\otimes|\phi^+_{2,2}\rangle_{a2b2c2d2}$. With a probability of $(1-F_c)^2$, the system is in the state of $|\psi^{c+}_{2,2}\rangle_{a1b1c1d1}\otimes|\psi^{c+}_{2,2}\rangle_{a2b2c2d2}$. With equal probability of $F_c(1-F_c)$, the system is in the state of $|\phi^+_{2,2}\rangle_{a1b1c1d1}\otimes|\psi^{c+}_{2,2}\rangle_{a2b2c2d2}$ or $|\psi^{c+}_{2,2}\rangle_{a1b1c1d1}\otimes|\phi^+_{2,2}\rangle_{a2b2c2d2}$.

For example, we first consider $|\phi^+_{2,2}\rangle_{a1b1c1d1}\otimes|\phi^+_{2,2}\rangle_{a2b2c2d2}$ with the probability of F_c^2. Combined with four resource states, the system is in $|\phi^+_{2,2}\rangle_{a1b1c1d1}|\phi^+_{2,2}\rangle_{a2b2c2d2}\otimes|\mathrm{GHZ_D}\rangle_{a3a4a5}|\mathrm{GHZ_D}\rangle_{b3b4b5}|\mathrm{GHZ_C}\rangle_{c3c4c5}|\mathrm{GHZ_C}\rangle_{d3d4d5}$. We list all items in a3b3c3d3 modes and their corresponding parity check results in Table 1. For the item $\frac{1}{\sqrt{2}}(|H,H,\alpha,\alpha\rangle+|V,V,-\alpha,-\alpha\rangle)_{a3b3c3d3}$, the corresponding state can be written as

$$
\begin{aligned}
&\tfrac{1}{\sqrt{2}}(|H,H,\alpha,\alpha\rangle_{a3b3c3d3}(|HH\rangle_{a4a1}|HH\rangle_{b4b1}|\alpha,\alpha\rangle_{c4c1}|\alpha,\alpha\rangle_{d4d1}|HH\rangle_{a5a2}|HH\rangle_{b5b2}|\alpha,\alpha\rangle_{c5c2}\\
&|\alpha,\alpha\rangle_{d5d2}|HH\rangle_{a4a1}|HH\rangle_{b4b1}|\alpha,\alpha\rangle_{c4c1}|\alpha,\alpha\rangle_{d4d1}|HV\rangle_{a5a2}|HV\rangle_{b5b2}|\alpha,-\alpha\rangle_{c5c2}|\alpha,-\alpha\rangle_{d5d2}\\
&|HV\rangle_{a4a1}|HV\rangle_{b4b1}|\alpha,-\alpha\rangle_{c4c1}|\alpha,-\alpha\rangle_{d4d1}|HH\rangle_{a5a2}|HH\rangle_{b5b2}|\alpha,\alpha\rangle_{c5c2}|\alpha,\alpha\rangle_{d5d2}\\
&|HV\rangle_{a4a1}|HV\rangle_{b4b1}|\alpha,-\alpha\rangle_{c4c1}|\alpha,-\alpha\rangle_{d4d1}|HV\rangle_{a5a2}|HV\rangle_{b5b2}|\alpha,-\alpha\rangle_{c5c2}|\alpha,-\alpha\rangle_{d5d2})\\
&+|V,V,-\alpha,-\alpha\rangle_{a3b3c3d3}(|VH\rangle_{a4a1}|VH\rangle_{b4b1}|-\alpha,\alpha\rangle_{c4c1}|-\alpha,\alpha\rangle_{d4d1}|VH\rangle_{a5a2}|VH\rangle_{b5b2}\\
&|-\alpha,\alpha\rangle_{c5c2}|-\alpha,\alpha\rangle_{d5d2}|VH\rangle_{a4a1}|VH\rangle_{b4b1}|-\alpha,\alpha\rangle_{c4c1}|-\alpha,\alpha\rangle_{d4d1}|VV\rangle_{a5a2}|VV\rangle_{b5b2}\\
&|-\alpha,-\alpha\rangle_{c5c2}|-\alpha,-\alpha\rangle_{d5d2}|VV\rangle_{a4a1}|VV\rangle_{b4b1}|-\alpha,-\alpha\rangle_{c4c1}|-\alpha,-\alpha\rangle_{d4d1}|VH\rangle_{a5a2}\\
&|VH\rangle_{b5b2}|-\alpha,\alpha\rangle_{c5c2}|-\alpha,\alpha\rangle_{d5d2}|VV\rangle_{a4a1}|VV\rangle_{b4b1}|-\alpha,-\alpha\rangle_{c4c1}|-\alpha,-\alpha\rangle_{d4d1}|VV\rangle_{a5a2}\\
&|VV\rangle_{b5b2}|-\alpha,-\alpha\rangle_{c5c2}|-\alpha,-\alpha\rangle_{d5d2})\\
\xrightarrow{\text{measurement}}\ &\tfrac{1}{\sqrt{2}}(|H,H,\alpha,\alpha\rangle+|V,V,-\alpha,-\alpha\rangle)_{a3b3c3d3}(|0^d0^d0^c0^c0^d0^d0^c0^c\rangle+|1^d1^d1^c1^c1^d1^d1^c1^c\rangle\\
&+|0^d0^d0^c0^c1^d1^d1^c1^c\rangle+|1^d1^d1^c1^c0^d0^d0^c0^c\rangle).
\end{aligned}
\tag{27}
$$

Table 1. The items in a3b3c3d3 modes of the state $|\phi^+_{2,2}\rangle_{a1b1c1d1}|\phi^+_{2,2}\rangle_{a2b2c2d2}|\mathrm{GHZ_D}\rangle_{a3a4a5}|\mathrm{GHZ_D}\rangle_{b3b4b5}\ |\mathrm{GHZ_C}\rangle_{c3c4c5}|\mathrm{GHZ_C}\rangle_{d3d4d5}$ and their corresponding measurement results and operations.

Parity check results	Items in a3b3c3d3 modes	Operations
$\|0^d0^d0^c0^c0^d0^d0^c0^c\rangle$, $\|1^d1^d1^c1^c1^d1^d1^c1^c\rangle$, $\|0^d0^d0^c0^c1^d1^d1^c1^c\rangle$, $\|1^d1^d1^c1^c0^d0^d0^c0^c\rangle$	$\frac{1}{\sqrt{2}}(\|H,H,\alpha,\alpha\rangle+\|V,V,-\alpha,-\alpha\rangle)_{a3b3c3d3}$	*IIII*
$\|0^d0^d0^c1^c0^d0^d0^c1^c\rangle$, $\|1^d1^d1^c0^c1^d1^d1^c0^c\rangle$, $\|0^d0^d0^c1^c1^d1^d1^c0^c\rangle$, $\|1^d1^d1^c0^c0^d0^d0^c1^c\rangle$	$\frac{1}{\sqrt{2}}(\|H,H,\alpha,-\alpha\rangle+\|V,V,-\alpha,\alpha\rangle)_{a3b3c3d3}$	*IIIX*
$\|0^d0^d1^c0^c0^d0^d1^c0^c\rangle$, $\|1^d1^d0^c1^c1^d1^d0^c1^c\rangle$, $\|0^d0^d1^c0^c1^d1^d0^c1^c\rangle$, $\|1^d1^d0^c1^c0^d0^d1^c0^c\rangle$	$\frac{1}{\sqrt{2}}(\|H,H,-\alpha,\alpha\rangle+\|V,V,\alpha,-\alpha\rangle)_{a3b3c3d3}$	*IIXI*
$\|0^d1^d0^c0^c0^d1^d0^c0^c\rangle$, $\|1^d0^d1^c1^c1^d0^d1^c1^c\rangle$, $\|0^d1^d0^c0^c1^d0^d1^c1^c\rangle$, $\|1^d0^d1^c1^c0^d1^d0^c0^c\rangle$	$\frac{1}{\sqrt{2}}(\|H,V,\alpha,\alpha\rangle+\|V,H,-\alpha,-\alpha\rangle)_{a3b3c3d3}$	*IXII*
$\|1^d0^d0^c0^c1^d0^d0^c0^c\rangle$, $\|0^d1^d1^c1^c0^d1^d1^c1^c\rangle$, $\|1^d0^d0^c0^c0^d1^d1^c1^c\rangle$, $\|0^d1^d1^c1^c1^d0^d0^c0^c\rangle$	$\frac{1}{\sqrt{2}}(\|V,H,\alpha,\alpha\rangle+\|H,V,-\alpha,-\alpha\rangle)_{a3b3c3d3}$	*XIII*
$\|0^d0^d1^c1^c0^d0^d1^c1^c\rangle$, $\|1^d1^d0^c0^c1^d1^d0^c0^c\rangle$, $\|0^d0^d1^c1^c1^d1^d0^c0^c\rangle$, $\|1^d1^d0^c0^c0^d0^d1^c1^c\rangle$	$\frac{1}{\sqrt{2}}(\|H,H,-\alpha,-\alpha\rangle+\|V,V,\alpha,\alpha\rangle)_{a3b3c3d3}$	*IIXX*
$\|0^d1^d0^c1^c0^d0^d0^c1^c\rangle$, $\|1^d0^d1^c0^c1^d0^d1^c0^c\rangle$, $\|0^d1^d0^c1^c1^d0^d1^c0^c\rangle$, $\|1^d0^d1^c0^c0^d1^d0^c1^c\rangle$	$\frac{1}{\sqrt{2}}(\|H,V,\alpha,-\alpha\rangle+\|V,H,-\alpha,\alpha\rangle)_{a3b3c3d3}$	*IXIX*
$\|1^d0^d0^c1^c1^d0^d0^c1^c\rangle$, $\|0^d1^d1^c0^c0^d1^d1^c0^c\rangle$, $\|1^d0^d0^c1^c0^d1^d1^c0^c\rangle$, $\|0^d1^d1^c0^c1^d0^d0^c1^c\rangle$	$\frac{1}{\sqrt{2}}(\|V,H,\alpha,-\alpha\rangle+\|H,V,-\alpha,\alpha\rangle)_{a3b3c3d3}$	*XIIX*

Therefore, by selecting four "proper cases" as $|0^d0^d0^c0^c0^d0^d0^c0^c\rangle$, $|1^d1^d1^c1^c1^d1^d1^c1^c\rangle$, $|0^d0^d0^c0^c1^d1^d1^c1^c\rangle$ and $|1^d1^d1^c1^c0^d0^d0^c0^c\rangle$, the parties can obtain the desired state $|\phi^+_{2,2}\rangle_{abcd}$. The other seven items in Table 1 have the similar structure, which can be obtained by selecting the corresponding "proper cases" and transformed to $|\phi^+_{2,2}\rangle_{abcd}$ by performing appropriate operations. Hence, these thirty-two types of "proper cases" in Table 1 can lead to the desired $|\phi^+_{2,2}\rangle_{abcd}$. Similarly, the parties can obtain $|\psi^{c+}_{2,2}\rangle_{abcd}$ from $|\psi^{c+}_{2,2}\rangle_{a1b1c1d1}\otimes|\psi^{c+}_{2,2}\rangle_{a2b2c2d2}$ with this selection principle. However, the crossed combinations $|\phi^+_{2,2}\rangle_{a1b1c1d1}\otimes|\psi^{c+}_{2,2}\rangle_{a2b2c2d2}$ and $|\psi^{c+}_{2,2}\rangle_{a1b1c1d1}\otimes|\phi^+_{2,2}\rangle_{a2b2c2d2}$ combined with the resource states can be automatically eliminated, for they never lead to the thirty-two "proper cases". Therefore, by selecting the "proper cases", the whole system evolves to

$$\rho^{c\prime}_{abcd}=F_c'|\phi^+_{2,2}\rangle_{abcd}\langle\phi^+_{2,2}|+(1-F_c')|\psi^{c+}_{2,2}\rangle_{abcd}\langle\psi^{c+}_{2,2}|, \tag{28}$$

with the success probability of $P_c=F_c^2+(1-F_c)^2$. Here, the new fidelity F_c' can be calculated as

$$F_c'=\frac{F_c^2}{F_c^2+(1-F_c)^2}. \tag{29}$$

On the other hand, assume that a bit-flip error occurs in the DV part with the probability of $1-F_{\rm d}$, the state $|\phi^+_{2,2}\rangle_{\rm abcd}$ becomes $|\psi^{\rm d+}_{2,2}\rangle_{\rm abcd}$ as

$$|\psi^{\rm d+}_{2,2}\rangle_{\rm abcd} = \frac{1}{\sqrt{2}}(|V,H,\alpha,\alpha\rangle_{\rm abcd} \pm |H,V,-\alpha,-\alpha\rangle_{\rm abcd}). \quad (30)$$

In this case, the hybrid state $|\phi^+_{2,2}\rangle_{\rm abcd}$ degrades to a mixed state with the form of

$$\rho^{\rm d}_{\rm abcd} = F_{\rm d}|\phi^+_{2,2}\rangle_{\rm abcd}\langle\phi^+_{2,2}| + (1-F_{\rm d})|\psi^{\rm d+}_{2,2}\rangle_{\rm abcd}\langle\psi^{\rm d+}_{2,2}|. \quad (31)$$

Two identical copies of such hybrid mixed states $\rho^{\rm d}_{\rm a1b1c1d1}$ and $\rho^{\rm d}_{\rm a2b2c2d2}$ are required to perform this MB-HEPP. Hence, the initial system $\rho^{\rm d}_{\rm a1b1c1d1}\otimes\rho^{\rm d}_{\rm a2b2c2d2}$ represents a probabilistic mixture of four hybrid pure states $|\phi^+_{2,2}\rangle_{\rm a1b1c1d1}\otimes|\phi^+_{2,2}\rangle_{\rm a2b2c2d2}$, $|\psi^{\rm d+}_{2,2}\rangle_{\rm a1b1c1d1}\otimes|\psi^{\rm d+}_{2,2}\rangle_{\rm a2b2c2d2}$, $|\phi^+_{2,2}\rangle_{\rm a1b1c1d1}\otimes|\psi^{\rm d+}_{2,2}\rangle_{\rm a2b2c2d2}$ and $|\psi^{\rm c+}_{2,2}\rangle_{\rm a1b1c1d1}\otimes|\phi^+_{2,2}\rangle_{\rm a2b2c2d2}$. By utilizing the apparatus in Fig. 3 and selecting the "proper cases", the state $|\phi^+_{2,2}\rangle_{\rm a1b1c1d1}\otimes|\phi^+_{2,2}\rangle_{\rm a2b2c2d2}$ and $|\psi^{\rm d+}_{2,2}\rangle_{\rm a1b1c1d1}\otimes|\psi^{\rm d+}_{2,2}\rangle_{\rm a2b2c2d2}$ collapse to $|\phi^+_{2,2}\rangle_{\rm abcd}$ and $|\psi^{\rm d+}_{2,2}\rangle_{\rm abcd}$, respectively. The two cross-combination states $|\phi^+_{2,2}\rangle_{\rm a1b1c1d1}\otimes|\psi^{\rm d+}_{2,2}\rangle_{\rm a2b2c2d2}$ and $|\psi^{\rm c+}_{2,2}\rangle_{\rm a1b1c1d1}\otimes|\phi^+_{2,2}\rangle_{\rm a2b2c2d2}$ can be automatically eliminated. Hence, they can achieve a new hybrid mixed state as

$$\rho^{\rm d\prime}_{\rm abcd} = F'_{\rm d}|\phi^+_{2,2}\rangle_{\rm abcd}\langle\phi^+_{2,2}| + (1-F'_{\rm d})|\psi^{\rm d+}_{2,2}\rangle_{\rm abcd}\langle\psi^{\rm d+}_{2,2}|, \quad (32)$$

with the success probability $P_{\rm d} = F^2_{\rm d} + (1-F_{\rm d})^2$. Here, the fidelity $F'_{\rm d}$ can be calculated as

$$F'_{\rm d} = \frac{F^2_{\rm d}}{F^2_{\rm d} + (1-F_{\rm d})^2}. \quad (33)$$

So far, we have discussed the case of $M=N=2$. By following the same steps, we can extend the MB-HEPP to the arbitrary case. In this scenario, we assume that a bit-flip error occurs in either the CV part or the DV part with a probability of $1-F_{{\rm c},M,N}$ or $1-F_{{\rm d},M,N}$, and the entire hybrid system evolves to

$$\begin{aligned}\rho^{\rm c}_{M,N} &= F_{{\rm c},M,N}|\phi^+_{M,N}\rangle_{M,N}\langle\phi^+_{M,N}| \\ &\quad + (1-F_{{\rm c},M,N})|\psi^{\rm c+}_{M,N}\rangle_{M,N}\langle\psi^{\rm c+}_{M,N}|, \end{aligned} \quad (34)$$

or

$$\begin{aligned}\rho^{\rm d}_{M,N} &= F_{{\rm d},M,N}|\phi^+_{M,N}\rangle_{M,N}\langle\phi^+_{M,N}| \\ &\quad + (1-F_{{\rm d},M,N})|\psi^{\rm d+}_{M,N}\rangle_{M,N}\langle\psi^{\rm d+}_{M,N}|. \end{aligned} \quad (35)$$

Here, $|\phi^+_{M,N}\rangle$, $|\psi^{\rm c+}_{M,N}\rangle$ and $|\psi^{\rm d+}_{M,N}\rangle$ are defined in Eqs. (21)–(23), respectively. The mixed states $\rho^{\rm c}_{M,N}$ and $\rho^{\rm d}_{M,N}$ can be purified by performing the MB-HEPP. Two identical mixed copies are required and the parties utilize $2M$ Md units and $2N$ Mc units to perform the parity checks. By selecting the "proper cases", the parties can finally obtain new mixed states as

$$\begin{aligned}\rho^{\rm c\prime}_{M,N} &= F'_{{\rm c},M,N}|\phi^+_{M,N}\rangle_{M,N}\langle\phi^+_{M,N}| \\ &\quad + (1-F'_{{\rm c},M,N})|\psi^{\rm c+}_{M,N}\rangle_{M,N}\langle\psi^{\rm c+}_{M,N}|, \\ \rho^{\rm d\prime}_{M,N} &= F'_{{\rm d},M,N}|\phi^+_{M,N}\rangle_{M,N}\langle\phi^+_{M,N}| \\ &\quad + (1-F'_{{\rm d},M,N})|\psi^{\rm d+}_{M,N}\rangle_{M,N}\langle\psi^{\rm d+}_{M,N}|, \end{aligned} \quad (36)$$

with the new fidelity

$$F'_{{\rm c},M,N} = \frac{F^2_{{\rm c},M,N}}{F^2_{{\rm c},M,N} + (1-F_{{\rm c},M,N})^2},$$
$$F'_{{\rm d},M,N} = \frac{F^2_{{\rm d},M,N}}{F^2_{{\rm d},M,N} + (1-F_{{\rm d},M,N})^2},$$

respectively. The success probabilities of this MB-HEPP are $P_{{\rm c},M,N} = F^2_{{\rm c},M,N} + (1-F_{{\rm c},M,N})^2$ and $P_{{\rm d},M,N} = F^2_{{\rm d},M,N} + (1-F_{{\rm d},M,N})^2$. If the initial fidelity satisfies $F_{{\rm c},M,N} > 1/2$ ($F_{{\rm d},M,N} > 1/2$), the parties can finally obtain a higher-quality hybrid entanglement with fidelity $F'_{{\rm c},M,N} > F_{{\rm c},M,N}$ ($F'_{{\rm d},M,N} > F_{{\rm d},M,N}$).

5. MB-HEPP under photon loss condition

In practical experimental conditions, besides decoherence, the coherent states inevitably suffer from photon loss during the transmission and operations, which will degrade the fidelity of entanglement and threaten the security of quantum protocols. To address this issue, it is crucial to correct the error of photon loss in coherent states before utilizing the entanglements. We take the hybrid Bell state $|\phi^+\rangle = \frac{1}{\sqrt{2}}(|H\rangle|\alpha\rangle + |V\rangle|-\alpha\rangle)$ as an example. Here, we employ a BS with the transmission coefficient of η to describe the photon loss model. Let's denote $|\beta\rangle = |\sqrt{\eta}\,\alpha\rangle$ and $|\gamma\rangle = |\sqrt{1-\eta}\,\alpha\rangle$. Consequently, the photon loss in the CV part transforms the initial state $|\phi^+\rangle$ to

$$|\phi^+_{\rm l}\rangle = \frac{1}{\sqrt{2}}(|H\rangle|\beta\rangle|\gamma\rangle + |V\rangle|-\beta\rangle|-\gamma\rangle)_{\rm abE}. \quad (37)$$

The other three Bell states in Eq. (1) degrade to

$$\begin{aligned}|\phi^-_{\rm l}\rangle &= \frac{1}{\sqrt{2}}(|H\rangle|\beta\rangle|\gamma\rangle - |V\rangle|-\beta\rangle|-\gamma\rangle)_{\rm abE}, \\ |\psi^\pm_{\rm l}\rangle &= \frac{1}{\sqrt{2}}(|H\rangle|-\beta\rangle|-\gamma\rangle \pm |V\rangle|\beta\rangle|\gamma\rangle)_{\rm abE}. \end{aligned} \quad (38)$$

The subscript Edenotes the photon loss in environment mode, while l represents the entangled state undergoing the photon loss. Similar to the above sections, we require two identical copies of mixed states to perform the MB-HEPP. In addition, the resource states for DV and CV parts are $|{\rm GHZ_D}\rangle$ and $|{\rm GHZ_C}\rangle$ in Eq. (3), respectively. Thus, the whole system is in the state of

$$\begin{aligned}&|\phi^+_{\rm l}\rangle_{\rm a1b1}|\phi^+_{\rm l}\rangle_{\rm a2b2}|{\rm GHZ_D}\rangle_{\rm d1d2d3}|{\rm GHZ_C}\rangle_{\rm c1c2c3} \\ &= \frac{1}{2\sqrt{2}N_3}(|H\rangle|\beta\rangle|\gamma\rangle + |V\rangle|-\beta\rangle|-\gamma\rangle)_{\rm a1b1E1} \\ &\quad\otimes(|H\rangle|\beta\rangle|\gamma\rangle + |V\rangle|-\beta\rangle|-\gamma\rangle)_{\rm a2b2E2} \\ &\quad\otimes(|HHH\rangle + |VVV\rangle)_{\rm d1d2d3} \\ &\quad\otimes(|\alpha,\alpha,\alpha\rangle + |-\alpha,-\alpha,-\alpha\rangle)_{\rm c1c2c3}. \end{aligned} \quad (39)$$

In this condition, for the CV part at Bob's side, after passing through the BS, the four combinations of coherent states evolve as

$$
\begin{aligned}
&|\alpha\rangle_{b1}|\beta\rangle_{c1}\xrightarrow{\text{Mc}}\left|\frac{1+\sqrt{\eta}}{\sqrt{2}}\alpha\right\rangle_{D4}\left|\frac{1-\sqrt{\eta}}{\sqrt{2}}\alpha\right\rangle_{D3}\rightarrow|0^{c}\rangle,\\
&|-\alpha\rangle_{b1}|-\beta\rangle_{c1}\xrightarrow{\text{Mc}}\left|\frac{-1-\sqrt{\eta}}{\sqrt{2}}\alpha\right\rangle_{D4}\left|\frac{-1+\sqrt{\eta}}{\sqrt{2}}\alpha\right\rangle_{D3}\rightarrow|0^{c}\rangle,\\
&|\alpha\rangle_{b1}|-\beta\rangle_{c1}\xrightarrow{\text{Mc}}\left|\frac{1-\sqrt{\eta}}{\sqrt{2}}\alpha\right\rangle_{D4}\left|\frac{1+\sqrt{\eta}}{\sqrt{2}}\alpha\right\rangle_{D3}\rightarrow|1^{c}\rangle,\\
&|-\alpha\rangle_{b1}|\beta\rangle_{c1}\xrightarrow{\text{Mc}}\left|\frac{-1+\sqrt{\eta}}{\sqrt{2}}\alpha\right\rangle_{D4}\left|\frac{-1-\sqrt{\eta}}{\sqrt{2}}\alpha\right\rangle_{D3}\rightarrow|1^{c}\rangle. \quad (40)
\end{aligned}
$$

We can observe that $|\alpha\rangle_{b1}|\beta\rangle_{c1}$ and $|-\alpha\rangle_{b1}|-\beta\rangle_{c1}$ leave most photons to the detector D4, while $|\alpha\rangle_{b1}|-\beta\rangle_{c1}$ and $|-\alpha\rangle_{b1}|\beta\rangle_{c1}$ leave most photons to the detector D3. In this way, these two parties can also be distinguished by detectors with the intensity measurement when α is sufficiently large. Therefore, for convenience, we also denote $|\alpha\rangle_{b1}|\beta\rangle_{c1}$ and $|-\alpha\rangle_{b1}|-\beta\rangle_{c1}$ as even-parity states, and $|\alpha\rangle_{b1}|-\beta\rangle_{c1}$ and $|-\alpha\rangle_{b1}|\beta\rangle_{c1}$ as odd-parity states. We present all parity check results of the noisy system in Table 2.

Now, with the method described in Ref. [66], we rewrite the environmental part of the above state in an orthogonal two-dimension basis $\{|u\rangle,|v\rangle\}$ as

$$
|\gamma\rangle_{E}=\mu_{E}|u\rangle_{E}+v_{E}|v\rangle_{E},\quad |-\gamma\rangle_{E}=\mu_{E}|u\rangle_{E}-v_{E}|v\rangle_{E}, \quad (41)
$$

where

$$
\mu_{E}=\sqrt{\frac{1+e^{-2\gamma^{2}}}{2}},\quad v_{E}=\sqrt{\frac{1-e^{-2\gamma^{2}}}{2}}. \quad (42)
$$

After we tracing over the loss modes E1E2 and performing appropriate operations in Table 2, the density matrix of the system can be expressed as

$$
(\mu_{E}^{4}+v_{E}^{4})|\phi^{+}\rangle_{d3c3}\langle\phi^{+}|+2\mu_{E}^{2}v_{E}^{2}|\phi^{-}\rangle_{d3c3}\langle\phi^{-}|. \quad (43)
$$

From Eq. (43), the photon loss error in $|\phi_{l}^{+}\rangle_{ab}$ is equal to the phase-flip error, which can be transformed to the bit-flip error state $|\psi^{+}\rangle_{d3c3}$ by applying Hadamard operations. Therefore, we can further purify this kind of error with our MB-HEPP in subsequent iterations.

Hence, after the MB-HEPP, the whole noisy hybrid state $|\phi_{l}^{+}\rangle_{a1b1}|\phi_{l}^{+}\rangle_{a2b2}$ evolves to

$$
\rho_{d3c3}^{l}=F_{l}|\phi^{+}\rangle_{d3c3}\langle\phi^{+}|+(1-F_{l})|\psi^{+}\rangle_{d3c3}\langle\psi^{+}|, \quad (44)
$$

where $F_{l}=\mu_{E}^{4}+v_{E}^{4}$.

Additionally, the bit-flip error under the photon loss condition can be described as

$$
\rho_{ab}^{lb}=F_{lb}|\phi_{l}^{+}\rangle_{ab}\langle\phi_{l}^{+}|+(1-F_{lb})|\psi_{l}^{+}\rangle_{ab}\langle\psi_{l}^{+}|. \quad (45)
$$

By applying the same procedure described above and tracing over the loss modes in the basis $\{|u\rangle,|v\rangle\}$, the whole hybrid system becomes

$$
\begin{aligned}
\rho_{d3c3}^{lb}=\;&N_{lb}\{F_{lb}^{2}[F_{l}|\phi^{+}\rangle_{d3c3}\langle\phi^{+}|+(1-F_{l})|\phi^{-}\rangle_{d3c3}\langle\phi^{-}|]\\
&+(1-F_{lb})^{2}[F_{l}|\psi^{+}\rangle_{d3c3}\langle\psi^{+}|\\
&+(1-F_{l})|\psi^{-}\rangle_{d3c3}\langle\psi^{-}|]\}, \quad (46)
\end{aligned}
$$

which incorporates both the bit-flip error and phase-flip error. Here, $N_{lb}=\frac{1}{F_{lb}^{2}+(1-F_{lb})^{2}}$ is the normalization factor. By implementing this MB-HEPP, the bit-flip error can be purified directly. However, the MB-HEPP cannot directly purify the phase-flip error. The parties can choose two copies of the distilled mixed states and convert the phase-flip error into the bit-flip error using Hadamard operations, and then purify it using this MB-HEPP. Consequently, the bit-flip error under the photon loss condition can also be addressed.

Table 2. The parity check results of the corresponding items in d3c3 modes of $|\phi_{l}^{+}\rangle_{a1b1}|\phi_{l}^{+}\rangle_{a2b2}|\text{GHZ}_{D}\rangle_{d1d2d3}|\text{GHZ}_{C}\rangle_{c1c2c3}$. The third column shows the states in d3c3 modes after tracing over the loss mode E1E2. The fourth column shows the corresponding operations.

parity	$\lvert\psi_{12}^{+}\rangle_{d3c3}$	$\text{Tr}_{E1E2}(\lvert\psi_{12}^{+}\rangle_{d3c3}\langle\psi_{12}^{+}\rvert)$	Operations
$\lvert 0^{d}0^{d}0^{c}0^{c}\rangle$	$\frac{1}{\sqrt{2}}(\lvert H\rangle\lvert\alpha\rangle\lvert\gamma\rangle\lvert\gamma\rangle+\lvert V\rangle\lvert-\alpha\rangle\lvert-\gamma\rangle\lvert-\gamma\rangle)_{d3c3E1E2}$		
$\lvert 0^{d}1^{d}0^{c}1^{c}\rangle$	$\frac{1}{\sqrt{2}}(\lvert H\rangle\lvert\alpha\rangle\lvert\gamma\rangle\lvert-\gamma\rangle+\lvert V\rangle\lvert-\alpha\rangle\lvert-\gamma\rangle\lvert\gamma\rangle)_{d3c3E1E2}$	$(\mu_{E}^{4}+v_{E}^{4})\lvert\phi^{+}\rangle_{d3c3}\langle\phi^{+}\rvert$	
$\lvert 1^{d}0^{d}1^{c}0^{c}\rangle$	$\frac{1}{\sqrt{2}}(\lvert H\rangle\lvert\alpha\rangle\lvert-\gamma\rangle\lvert\gamma\rangle+\lvert V\rangle\lvert-\alpha\rangle\lvert\gamma\rangle\lvert-\gamma\rangle)_{d3c3E1E2}$	$+2\mu_{E}^{2}v_{E}^{2}\lvert\phi^{-}\rangle_{d3c3}\langle\phi^{-}\rvert$	II
$\lvert 1^{d}1^{d}1^{c}1^{c}\rangle$	$\frac{1}{\sqrt{2}}(\lvert H\rangle\lvert\alpha\rangle\lvert-\gamma\rangle\lvert-\gamma\rangle+\lvert V\rangle\lvert-\alpha\rangle\lvert\gamma\rangle\lvert\gamma\rangle)_{d3c3E1E2}$		
$\lvert 0^{d}0^{d}1^{c}1^{c}\rangle$	$\frac{1}{\sqrt{2}}(\lvert H\rangle\lvert-\alpha\rangle\lvert\gamma\rangle\lvert\gamma\rangle+\lvert V\rangle\lvert\alpha\rangle\lvert-\gamma\rangle\lvert-\gamma\rangle)_{d3c3E1E2}$		
$\lvert 0^{d}1^{d}1^{c}0^{c}\rangle$	$\frac{1}{\sqrt{2}}(\lvert H\rangle\lvert-\alpha\rangle\lvert\gamma\rangle\lvert-\gamma\rangle+\lvert V\rangle\lvert\alpha\rangle\lvert-\gamma\rangle\lvert\gamma\rangle)_{d3c3E1E2}$	$(\mu_{E}^{4}+v_{E}^{4})\lvert\psi^{+}\rangle_{d3c3}\langle\psi^{+}\rvert$	
$\lvert 1^{d}0^{d}0^{c}1^{c}\rangle$	$\frac{1}{\sqrt{2}}(\lvert H\rangle\lvert-\alpha\rangle\lvert-\gamma\rangle\lvert\gamma\rangle+\lvert V\rangle\lvert\alpha\rangle\lvert\gamma\rangle\lvert-\gamma\rangle)_{d3c3E1E2}$	$+2\mu_{E}^{2}v_{E}^{2}\lvert\psi^{-}\rangle_{d3c3}\langle\psi^{-}\rvert$	IX or XI
$\lvert 1^{d}1^{d}0^{c}0^{c}\rangle$	$\frac{1}{\sqrt{2}}(\lvert H\rangle\lvert-\alpha\rangle\lvert-\gamma\rangle\lvert-\gamma\rangle+\lvert V\rangle\lvert\alpha\rangle\lvert\gamma\rangle\lvert\gamma\rangle)_{d3c3E1E2}$		

6. Discussion and conclusion

In the paper, we first discuss an MB-HEPP for a single bit-flip error whether in the CV part or the DV part. Furthermore, we extend our MB-HEPP to the multi-copy and multi-party scenarios, and further consider the photon-loss condition. In addition to the bit-flip error, the phase-flip error may also occur. The MB-HEPP cannot directly purify the phase-flip error. However, the parties can first convert the phase-flip error into the bit-flip error, and then purify the bit-flip error in the next purification round.[55]

To implement our MB-HEPP, it is essential to simultaneously prepare at least two pairs of HESs and two types of re-

source GHZ states. As demonstrated in Ref. [28], such HESs can be generated by interfering a polarization entangled photon pair and coherent states using a series BSs and a PBS. Hence, the experimental generation of multiple pairs of HESs can be designed by cascading multiple setups in Ref. [28], or by time multiplexing a single setup. For the generation of polarization GHZ state, one can employ the traditional linear optical method[67] or use the QND method[68] to achieve a higher success probability. On the other hand, one can generate the coherent GHZ state in a probabilistic way similar to DV, or accomplish it without photon counting.[69]

In this MB-HEPP, we replace the BSM in common MB-EPPs[63,64] with the parity check. As the linear optical BSM can only distinguish two of the four Bell states, its success probability is only 50%. However, the success probability of the parity check is 100%. As a result, the adoption of the parity check can effectively increase the total success probability of the MB-HEPP. In detail, in the MB-HEPP for the two-copy hybrid Bell states, the adoption of the parity check can increase the success probability to 8 times that in the MB-HEPP with BSM. In the ME-HEPPs for N-copy hybrid Bell states and multi-partite hybrid entangled state $|\phi^{\pm}_{M,N}\rangle$, the adoption of the parity check can increase the success probabilities to 2^{N+1} and 2^{N+M+1} times those with BSM, respectively.

In conclusion, we propose an optical MB-HEPP for the two-party and multi-party HESs which consist of polarization photons and coherent states. In this protocol, we first address the purification of the bit-flip error and phase-flip error in the basic two-party HES. Subsequently, we extend this MB-HEPP to the multi-copy scenario, which utilizes multiple low-quality HES copies to distill a higher-quality HES in one iteration. Furthermore, the MB-HEPP protocol for the multi-party HES has been proposed. For the photon-loss error in coherent states, we can transform it to the phase-flip error by using another set of orthogonal basis $\{|u\rangle, |v\rangle\}$ and purify it with this MB-HEPP protocol. Compared with previous HEPPs, our MB-HEPP protocol has several advantages. First, it does not depend on the post-selection and the purified HESs can be retained for further application. Second, this protocol does not require the BSM, but only requires the parity check, which makes this protocol have higher success probability and more feasible. This MB-HEPP has the potential to contribute to future HES-based technologies and realization of heterogeneous quantum networks.

Appendix A: The detailed analysis of the MB-HEPP for two-copy hybrid Bell states

In this appendix, we provide the detailed analysis of our MB-HEPP for two-copy hybrid Bell states ρ_{a1b1} and ρ_{a2b2}. With a probability of F^2, the system is in the state of $|\phi^+\rangle_{\mathrm{a1b1}} \otimes |\phi^+\rangle_{\mathrm{a2b2}}$. With a probability of $(1-F)^2$, the system is in the state of $|\psi^+\rangle_{\mathrm{a1b1}} \otimes |\psi^+\rangle_{\mathrm{a2b2}}$. With equal probability of $F(1-F)$, the system is in the state of $|\phi^+\rangle_{\mathrm{a1b1}} \otimes |\psi^+\rangle_{\mathrm{a2b2}}$ or $|\psi^+\rangle_{\mathrm{a1b1}} \otimes |\phi^+\rangle_{\mathrm{a2b2}}$.

We first analyze the case of $|\phi^+\rangle_{\mathrm{a1b1}} \otimes |\phi^+\rangle_{\mathrm{a2b2}}$. Therefore, with the probability of F^2, the state $\rho_{\mathrm{a1b1}} \otimes \rho_{\mathrm{a2b2}} \otimes |\mathrm{GHZ_D}\rangle_{\mathrm{d1d2d3}} \otimes |\mathrm{GHZ_C}\rangle_{\mathrm{c1c2c3}}$ can be simplified as

$$
\begin{aligned}
&|\phi^+\rangle_{\mathrm{a1b1}}|\phi^+\rangle_{\mathrm{a2b2}}|\mathrm{GHZ_D}\rangle_{\mathrm{d1d2d3}}|\mathrm{GHZ_C}\rangle_{\mathrm{c1c2c3}} \\
&= \frac{1}{2\sqrt{2}N_3}|H,\alpha\rangle_{\mathrm{d3c3}}(|HH\rangle_{\mathrm{d1a1}}|HH\rangle_{\mathrm{d2a2}}|\alpha,\alpha\rangle_{\mathrm{c1b1}}|\alpha,\alpha\rangle_{\mathrm{c2b2}} + |HH\rangle_{\mathrm{d1a1}}|HV\rangle_{\mathrm{d2a2}}|\alpha,\alpha\rangle_{\mathrm{c1b1}}|\alpha,-\alpha\rangle_{\mathrm{c2b2}} \\
&\quad + |HV\rangle_{\mathrm{d1a1}}|HH\rangle_{\mathrm{d2a2}}|\alpha,-\alpha\rangle_{\mathrm{c1b1}}|\alpha,\alpha\rangle_{\mathrm{c2b2}} + |HV\rangle_{\mathrm{d1a1}}|HV\rangle_{\mathrm{d2a2}}|\alpha,-\alpha\rangle_{\mathrm{c1b1}}|\alpha,-\alpha\rangle_{\mathrm{c2b2}}) \\
&\quad + \frac{1}{2\sqrt{2}N_3}|H,-\alpha\rangle_{\mathrm{d3c3}}(|HH\rangle_{\mathrm{d1a1}}|HH\rangle_{\mathrm{d2a2}}|-\alpha,\alpha\rangle_{\mathrm{c1b1}}|-\alpha,\alpha\rangle_{\mathrm{c2b2}} + |HH\rangle_{\mathrm{d1a1}}|HV\rangle_{\mathrm{d2a2}}|-\alpha,\alpha\rangle_{\mathrm{c1b1}}|-\alpha,-\alpha\rangle_{\mathrm{c2b2}} \\
&\quad + |HV\rangle_{\mathrm{d1a1}}|HH\rangle_{\mathrm{d2a2}}|-\alpha,-\alpha\rangle_{\mathrm{c1b1}}|-\alpha,\alpha\rangle_{\mathrm{c2b2}} + |HV\rangle_{\mathrm{d1a1}}|HV\rangle_{\mathrm{d2a2}}|-\alpha,-\alpha\rangle_{\mathrm{c1b1}}|-\alpha,-\alpha\rangle_{\mathrm{c2b2}}) \\
&\quad + \frac{1}{2\sqrt{2}N_3}|V,\alpha\rangle_{\mathrm{d3c3}}(|VH\rangle_{\mathrm{d1a1}}|VH\rangle_{\mathrm{d2a2}}|\alpha,\alpha\rangle_{\mathrm{c1b1}}|\alpha,\alpha\rangle_{\mathrm{c2b2}} + |VH\rangle_{\mathrm{d1a1}}|VV\rangle_{\mathrm{d2a2}}|\alpha,\alpha\rangle_{\mathrm{c1b1}}|\alpha,-\alpha\rangle_{\mathrm{c2b2}} \\
&\quad + |VV\rangle_{\mathrm{d1a1}}|VH\rangle_{\mathrm{d2a2}}|\alpha,-\alpha\rangle_{\mathrm{c1b1}}|\alpha,\alpha\rangle_{\mathrm{c2b2}} + |VV\rangle_{\mathrm{d1a1}}|VV\rangle_{\mathrm{d2a2}}|\alpha,-\alpha\rangle_{\mathrm{c1b1}}|\alpha,-\alpha\rangle_{\mathrm{c2b2}}) \\
&\quad + \frac{1}{2\sqrt{2}N_3}|V,-\alpha\rangle_{\mathrm{d3c3}}(|VH\rangle_{\mathrm{d1a1}}|VH\rangle_{\mathrm{d2a2}}|-\alpha,\alpha\rangle_{\mathrm{c1b1}}|-\alpha,\alpha\rangle_{\mathrm{c2b2}} + |VH\rangle_{\mathrm{d1a1}}|VV\rangle_{\mathrm{d2a2}}|-\alpha,\alpha\rangle_{\mathrm{c1b1}}|-\alpha,-\alpha\rangle_{\mathrm{c2b2}} \\
&\quad + |VV\rangle_{\mathrm{d1a1}}|VH\rangle_{\mathrm{d2a2}}|-\alpha,-\alpha\rangle_{\mathrm{c1b1}}|-\alpha,\alpha\rangle_{\mathrm{c2b2}} + |VV\rangle_{\mathrm{d1a1}}|VV\rangle_{\mathrm{d2a2}}|-\alpha,-\alpha\rangle_{\mathrm{c1b1}}|-\alpha,-\alpha\rangle_{\mathrm{c2b2}}) \\
&\xrightarrow{\text{measure}} \frac{1}{2\sqrt{2}N_3}(|H,\alpha\rangle_{\mathrm{d3c3}} + |V,-\alpha\rangle_{\mathrm{d3c3}})(|0^{\mathrm{d}}0^{\mathrm{d}}0^{\mathrm{c}}0^{\mathrm{c}}\rangle + |0^{\mathrm{d}}1^{\mathrm{d}}0^{\mathrm{c}}1^{\mathrm{c}}\rangle + |1^{\mathrm{d}}0^{\mathrm{d}}1^{\mathrm{c}}0^{\mathrm{c}}\rangle + |1^{\mathrm{d}}1^{\mathrm{d}}1^{\mathrm{c}}1^{\mathrm{c}}\rangle) \\
&\quad + \frac{1}{2\sqrt{2}N_3}(|H,-\alpha\rangle_{\mathrm{d3c3}} + |V,\alpha\rangle_{\mathrm{d3c3}})(|0^{\mathrm{d}}0^{\mathrm{d}}1^{\mathrm{c}}1^{\mathrm{c}}\rangle + |0^{\mathrm{d}}1^{\mathrm{d}}1^{\mathrm{c}}0^{\mathrm{c}}\rangle + |1^{\mathrm{d}}0^{\mathrm{d}}0^{\mathrm{c}}1^{\mathrm{c}}\rangle + |1^{\mathrm{d}}1^{\mathrm{d}}0^{\mathrm{c}}0^{\mathrm{c}}\rangle). \qquad \text{(A1)}
\end{aligned}
$$

Hence, after Alice and Bob performing the parity check and selecting the result $|0^{\mathrm{d}}0^{\mathrm{d}}0^{\mathrm{c}}0^{\mathrm{c}}\rangle$, $|0^{\mathrm{d}}1^{\mathrm{d}}0^{\mathrm{c}}1^{\mathrm{c}}\rangle$, $|1^{\mathrm{d}}0^{\mathrm{d}}1^{\mathrm{c}}0^{\mathrm{c}}\rangle$ or $|1^{\mathrm{d}}1^{\mathrm{d}}1^{\mathrm{c}}1^{\mathrm{c}}\rangle$, they can obtain the desired state in modes d3c3 as

$$
|\phi^+\rangle_{\mathrm{d3c3}} = \frac{1}{\sqrt{2}}(|H\rangle|\alpha\rangle + |V\rangle|-\alpha\rangle)_{\mathrm{d3c3}}. \qquad \text{(A2)}
$$

If their measurement result is $|0^{\rm d}0^{\rm d}1^{\rm c}1^{\rm c}\rangle$, $|0^{\rm d}1^{\rm d}1^{\rm c}0^{\rm c}\rangle$, $|1^{\rm d}0^{\rm d}0^{\rm c}1^{\rm c}\rangle$ or $|1^{\rm d}1^{\rm d}0^{\rm c}0^{\rm c}\rangle$, the state of the remaining photons in modes d3c3 becomes

$$|\psi^+\rangle_{\rm d3c3}=\frac{1}{\sqrt{2}}(|H\rangle|-\alpha\rangle+|V\rangle|\alpha\rangle)_{\rm d3c3}, \tag{A3}$$

which can be transformed to the desired state $|\phi^+\rangle_{\rm d3c3}$ by performing a bit-flip operation on a random qubit.

Similarly, with the probability $(1-F)^2$, the system can be simplified as

$$\begin{aligned}
&|\psi^+\rangle_{\rm a1b1}|\psi^+\rangle_{\rm a2b2}|{\rm GHZ_D}\rangle_{\rm d1d2d3}|{\rm GHZ_C}\rangle_{\rm c1c2c3}\\
=&\frac{1}{2\sqrt{2}N_3}|H,\alpha\rangle_{\rm d3c3}(|HH\rangle_{\rm d1a1}|HH\rangle_{\rm d2a2}|\alpha,-\alpha\rangle_{\rm c1b1}|\alpha,-\alpha\rangle_{\rm c2b2}+|HH\rangle_{\rm d1a1}|HV\rangle_{\rm d2a2}|\alpha,-\alpha\rangle_{\rm c1b1}|\alpha,\alpha\rangle_{\rm c2b2}\\
&+|HV\rangle_{\rm d1a1}|HH\rangle_{\rm d2a2}|\alpha,\alpha\rangle_{\rm c1b1}|\alpha,-\alpha\rangle_{\rm c2b2}+|HV\rangle_{\rm d1a1}|HV\rangle_{\rm d2a2}|\alpha,\alpha\rangle_{\rm c1b1}|\alpha,\alpha\rangle_{\rm c2b2})\\
&+\frac{1}{2\sqrt{2}N_3}|H,-\alpha\rangle_{\rm d3c3}(|HH\rangle_{\rm d1a1}|HH\rangle_{\rm d2a2}|-\alpha,-\alpha\rangle_{\rm c1b1}|-\alpha,-\alpha\rangle_{\rm c2b2}+|HH\rangle_{\rm d1a1}|HV\rangle_{\rm d2a2}|-\alpha,-\alpha\rangle_{\rm c1b1}|-\alpha,\alpha\rangle_{\rm c2b2}\\
&+|HV\rangle_{\rm d1a1}|HH\rangle_{\rm d2a2}|-\alpha,\alpha\rangle_{\rm c1b1}|-\alpha,-\alpha\rangle_{\rm c2b2}+|HV\rangle_{\rm d1a1}|HV\rangle_{\rm d2a2}|-\alpha,\alpha\rangle_{\rm c1b1}|-\alpha,\alpha\rangle_{\rm c2b2})\\
&+\frac{1}{2\sqrt{2}N_3}|V,\alpha\rangle_{\rm d3c3}(|VH\rangle_{\rm d1a1}|VH\rangle_{\rm d2a2}|\alpha,-\alpha\rangle_{\rm c1b1}|\alpha,-\alpha\rangle_{\rm c2b2}+|VH\rangle_{\rm d1a1}|VV\rangle_{\rm d2a2}|\alpha,-\alpha\rangle_{\rm c1b1}|\alpha,\alpha\rangle_{\rm c2b2}\\
&+|VV\rangle_{\rm d1a1}|VH\rangle_{\rm d2a2}|\alpha,\alpha\rangle_{\rm c1b1}|\alpha,-\alpha\rangle_{\rm c2b2}+|VV\rangle_{\rm d1a1}|VV\rangle_{\rm d2a2}|\alpha,\alpha\rangle_{\rm c1b1}|\alpha,\alpha\rangle_{\rm c2b2})\\
&+\frac{1}{2\sqrt{2}N_3}|V,-\alpha\rangle_{\rm d3c3}(|VH\rangle_{\rm d1a1}|VH\rangle_{\rm d2a2}|-\alpha,-\alpha\rangle_{\rm c1b1}|-\alpha,-\alpha\rangle_{\rm c2b2}+|VH\rangle_{\rm d1a1}|VV\rangle_{\rm d2a2}|-\alpha,-\alpha\rangle_{\rm c1b1}|-\alpha,\alpha\rangle_{\rm c2b2}\\
&+|VV\rangle_{\rm d1a1}|VH\rangle_{\rm d2a2}|-\alpha,\alpha\rangle_{\rm c1b1}|-\alpha,-\alpha\rangle_{\rm c2b2}+|VV\rangle_{\rm d1a1}|VV\rangle_{\rm d2a2}|-\alpha,\alpha\rangle_{\rm c1b1}|-\alpha,\alpha\rangle_{\rm c2b2})\\
\xrightarrow{\text{measure}}&\frac{1}{2\sqrt{2}N_3}(|H,-\alpha\rangle_{\rm d3c3}+|V,\alpha\rangle_{\rm d3c3})(|0^{\rm d}0^{\rm d}0^{\rm c}0^{\rm c}\rangle+|0^{\rm d}1^{\rm d}0^{\rm c}1^{\rm c}\rangle+|1^{\rm d}0^{\rm d}1^{\rm c}0^{\rm c}\rangle+|1^{\rm d}1^{\rm d}1^{\rm c}1^{\rm c}\rangle)\\
&+\frac{1}{2\sqrt{2}N_3}(|H,\alpha\rangle_{\rm d3c3}+|V,-\alpha\rangle_{\rm d3c3})(|0^{\rm d}0^{\rm d}1^{\rm c}1^{\rm c}\rangle+|0^{\rm d}1^{\rm d}1^{\rm c}0^{\rm c}\rangle+|1^{\rm d}0^{\rm d}0^{\rm c}1^{\rm c}\rangle+|1^{\rm d}1^{\rm d}0^{\rm c}0^{\rm c}\rangle).
\end{aligned} \tag{A4}$$

Therefore, by selecting $|0^{\rm d}0^{\rm d}0^{\rm c}0^{\rm c}\rangle$, $|0^{\rm d}1^{\rm d}0^{\rm c}1^{\rm c}\rangle$, $|0^{\rm d}1^{\rm d}0^{\rm c}1^{\rm c}\rangle$ or $|1^{\rm d}1^{\rm d}1^{\rm c}1^{\rm c}\rangle$, Alice and Bob can obtain

$$|\psi^+\rangle_{\rm d3c3}=\frac{1}{\sqrt{2}}(|H\rangle|-\alpha\rangle+|V\rangle|\alpha\rangle)_{\rm d3c3}. \tag{A5}$$

Otherwise, if they select $|0^{\rm d}0^{\rm d}1^{\rm c}1^{\rm c}\rangle$, $|0^{\rm d}1^{\rm d}1^{\rm c}0^{\rm c}\rangle$, $|1^{\rm d}0^{\rm d}0^{\rm c}1^{\rm c}\rangle$ or $|1^{\rm d}1^{\rm d}0^{\rm c}0^{\rm c}\rangle$, the system becomes

$$|\phi^+\rangle_{\rm d3c3}=\frac{1}{\sqrt{2}}(|H\rangle|\alpha\rangle+|V\rangle|-\alpha\rangle)_{\rm d3c3}, \tag{A6}$$

which will be transformed into $|\psi^+\rangle_{\rm d3c3}$ through a bit-flip operation.

The crossed combinations $|\phi^+\rangle_{\rm a1b1}|\psi^+\rangle_{\rm a2b2}$ and $|\psi^+\rangle_{\rm a1b1}|\phi^+\rangle_{\rm a2b2}$ of $\rho_{\rm a1b1}\otimes\rho_{\rm a2b2}$ combined with $|{\rm GHZ_D}\rangle_{\rm d1d2d3}$ $|{\rm GHZ_C}\rangle_{\rm c1c2c3}$ can be automatically eliminated. For example, the state $|\phi^+\rangle_{\rm a1b1}|\psi^+\rangle_{\rm a2b2}$ combined with $|{\rm GHZ_D}\rangle_{\rm d1d2d3}|{\rm GHZ_C}\rangle_{\rm c1c2c3}$ can be written as

$$\begin{aligned}
&|\phi^+\rangle_{\rm a1b1}|\psi^+\rangle_{\rm a2b2}|{\rm GHZ_D}\rangle_{\rm d1d2d3}|{\rm GHZ_C}\rangle_{\rm c1c2c3}\\
=&\frac{1}{2\sqrt{2}N_3}|H,\alpha\rangle_{\rm d3c3}(|HH\rangle_{\rm d1a1}|HH\rangle_{\rm d2a2}|\alpha,\alpha\rangle_{\rm c1b1}|\alpha,-\alpha\rangle_{\rm c2b2}+|HH\rangle_{\rm d1a1}|HV\rangle_{\rm d2a2}|\alpha,\alpha\rangle_{\rm c1b1}|\alpha,\alpha\rangle_{\rm c2b2}\\
&+|HV\rangle_{\rm d1a1}|HH\rangle_{\rm d2a2}|\alpha,-\alpha\rangle_{\rm c1b1}|\alpha,-\alpha\rangle_{\rm c2b2}+|HV\rangle_{\rm d1a1}|HV\rangle_{\rm d2a2}|\alpha,-\alpha\rangle_{\rm c1b1}|\alpha,\alpha\rangle_{\rm c2b2})\\
&+\frac{1}{2\sqrt{2}N_3}|H,-\alpha\rangle_{\rm d3c3}(|HH\rangle_{\rm d1a1}|HH\rangle_{\rm d2a2}|-\alpha,\alpha\rangle_{\rm c1b1}|-\alpha,-\alpha\rangle_{\rm c2b2}+|HH\rangle_{\rm d1a1}|HV\rangle_{\rm d2a2}|-\alpha,\alpha\rangle_{\rm c1b1}|-\alpha,\alpha\rangle_{\rm c2b2}\\
&+|HV\rangle_{\rm d1a1}|HH\rangle_{\rm d2a2}|-\alpha,-\alpha\rangle_{\rm c1b1}|-\alpha,-\alpha\rangle_{\rm c2b2}+|HV\rangle_{\rm d1a1}|HV\rangle_{\rm d2a2}|-\alpha,-\alpha\rangle_{\rm c1b1}|-\alpha,\alpha\rangle_{\rm c2b2})\\
&+\frac{1}{2\sqrt{2}N_3}|V,\alpha\rangle_{\rm d3c3}(|VH\rangle_{\rm d1a1}|VH\rangle_{\rm d2a2}|\alpha,\alpha\rangle_{\rm c1b1}|\alpha,-\alpha\rangle_{\rm c2b2}+|VH\rangle_{\rm d1a1}|VV\rangle_{\rm d2a2}|\alpha,\alpha\rangle_{\rm c1b1}|\alpha,\alpha\rangle_{\rm c2b2}\\
&+|VV\rangle_{\rm d1a1}|VH\rangle_{\rm d2a2}|\alpha,-\alpha\rangle_{\rm c1b1}|\alpha,-\alpha\rangle_{\rm c2b2}+|VV\rangle_{\rm d1a1}|VV\rangle_{\rm d2a2}|\alpha,-\alpha\rangle_{\rm c1b1}|\alpha,\alpha\rangle_{\rm c2b2})\\
&+\frac{1}{2\sqrt{2}N_3}|V,-\alpha\rangle_{\rm d3c3}(|VH\rangle_{\rm d1a1}|VH\rangle_{\rm d2a2}|-\alpha,\alpha\rangle_{\rm c1b1}|-\alpha,-\alpha\rangle_{\rm c2b2}+|VH\rangle_{\rm d1a1}|VV\rangle_{\rm d2a2}|-\alpha,\alpha\rangle_{\rm c1b1}|-\alpha,\alpha\rangle_{\rm c2b2}\\
&+|VV\rangle_{\rm d1a1}|VH\rangle_{\rm d2a2}|-\alpha,-\alpha\rangle_{\rm c1b1}|-\alpha,-\alpha\rangle_{\rm c2b2}+|VV\rangle_{\rm d1a1}|VV\rangle_{\rm d2a2}|-\alpha,-\alpha\rangle_{\rm c1b1}|-\alpha,\alpha\rangle_{\rm c2b2})
\end{aligned}$$

$$\xrightarrow{\text{measure}} \frac{1}{2\sqrt{2}N_3}(|H,\alpha\rangle_{\text{d3c3}}+|V,-\alpha\rangle_{\text{d3c3}})(|0^{\text{d}}0^{\text{d}}0^{\text{c}}1^{\text{c}}\rangle+|0^{\text{d}}1^{\text{d}}0^{\text{c}}0^{\text{c}}\rangle+|1^{\text{d}}0^{\text{d}}1^{\text{c}}1^{\text{c}}\rangle+|1^{\text{d}}1^{\text{d}}1^{\text{c}}0^{\text{c}}\rangle)$$
$$+\frac{1}{2\sqrt{2}N_3}(|H,-\alpha\rangle_{\text{d3c3}}+|V,\alpha\rangle_{\text{d3c3}})(|0^{\text{d}}0^{\text{d}}1^{\text{c}}0^{\text{c}}\rangle+|0^{\text{d}}1^{\text{d}}1^{\text{c}}1^{\text{c}}\rangle+|1^{\text{d}}0^{\text{d}}0^{\text{c}}0^{\text{c}}\rangle+|1^{\text{d}}1^{\text{d}}0^{\text{c}}1^{\text{c}}\rangle), \tag{A7}$$

which could only lead to 8 different parity check results $|0^{\text{d}}0^{\text{d}}0^{\text{c}}1^{\text{c}}\rangle$, $|0^{\text{d}}1^{\text{d}}0^{\text{c}}0^{\text{c}}\rangle$, $|1^{\text{d}}0^{\text{d}}1^{\text{c}}1^{\text{c}}\rangle$, $|1^{\text{d}}1^{\text{d}}1^{\text{c}}0^{\text{c}}\rangle$, $|0^{\text{d}}0^{\text{d}}1^{\text{c}}0^{\text{c}}\rangle$, $|0^{\text{d}}1^{\text{d}}1^{\text{c}}1^{\text{c}}\rangle$, $|1^{\text{d}}0^{\text{d}}0^{\text{c}}0^{\text{c}}\rangle$ and $|1^{\text{d}}1^{\text{d}}0^{\text{c}}1^{\text{c}}\rangle$.

Acknowledgements

Project supported by the National Natural Science Foundation of China (Grant Nos. 12175106 and 92365110) and the Postgraduate Research and Practice Innovation Program of Jiangsu Province (Grant No. KYCX23-1028).

References

[1] Bennett C H, Brassard G, Crépeau C, Jozsa R, Peres A and Wootters W K 1993 *Phys. Rev. Lett.* **70** 1895
[2] Ekert A K 1991 *Phys. Rev. Lett.* **67** 661
[3] Long G L and Liu X S 2002 *Phys. Rev. A* **65** 032302
[4] Deng F G, Long G L and Liu X S 2003 *Phys. Rev. A* **68** 042317
[5] Sheng Y B, Zhou L and Long G L 2022 *Sci. Bull.* **67** 367
[6] Ying J W, Zhou L, Zhong W and Sheng Y B 2022 *Chin. Phys. B* **31** 120303
[7] Hillery M, Bužek V and Berthiaume A 1999 *Phys. Rev. A* **59** 1829
[8] Zhang Q, Zhong W, Du M M, Shen S T, Li X Y, Zhang A L, Zhou L, and Sheng Y B 2024 *Phys. Rev. A* **110** 042403
[9] Briegel H J, Dür W, Cirac J I and Zoller P 1998 *Phys. Rev. Lett.* **81** 5932
[10] Bernardes N K, Praxmeyer L and van Loock P 2011 *Phys. Rev. A* **83** 012323
[11] Bergmann M and van Loock P 2019 *Phys. Rev. A* **99** 032349
[12] Beals R, Brierley S, Gray O, Harrow A W, Kutin S, Linden N, Shepherd D and Stather M 2013 *Proc. Math. Phys. Eng. Sci.* **469** 20120686
[13] Wang J, Sciarrino F, Laing A and Thompson M G 2020 *Nat. Photonics* **14** 273
[14] Krelina M 2021 *EPJ Quantum Technol.* **8** 24
[15] Pelucchi E, Fagas G, Aharonovich I, Englund D, Figueroa E, Gong Q, Hannes H, Liu J, Lu C Y and Matsuda N 2022 *Nat. Rev. Phys.* **4** 194
[16] Krenn M, Landgraf J, Foesel T and Marquardt F 2023 *Phys. Rev. A* **107** 010101
[17] Li S W, Feng T F, Hu X L and Zhou X Q 2023 *Chin. Phys. B* **32** 104214
[18] Zhu P H, Zhong W, Du M M, Li X Y, Zhou L and Sheng Y B 2024 *Chin. Phys. B* **33** 030302
[19] Fan J H, Xia P W, Dai D K and Chen Y X 2024 *Chin. Phys. B* **32** 120304
[20] Jeong H, Zavatta A, Kang M, Lee S W, Costanzo L S, Grandi S, Ralph T C and Bellini M 2014 *Nat. Photonics* **8** 564
[21] van Loock P 2011 *Laser Photonics Rev.* **5** 167
[22] Jing B, Wang X J, Yu Y, Sun P F, Jiang Y, Yang S J, Jiang W H, Luo X Y, Zhang J, Jiang X, Bao X H and Pan J W 2019 *Nat. Photonics* **13** 210
[23] Reiserer A and Rempe G 2015 *Rev. Mod. Phys.* **87** 1379
[24] Cattaneo M, Paris M G and Olivares S 2018 *Phys. Rev. A* **98** 012333
[25] Guccione G, Darras T, Le Jeannic H, Verma V B, Nam S W, Cavaillès A and Laurat J 2020 *Sci. Adv.* **6** eaba4508
[26] Omkar S, Teo Y S, Lee S W and Jeong H 2021 *Phys. Rev. A* **103** 032602
[27] Andersen U L, Neergaard-Nielsen J S, van Loock P and Furusawa A 2015 *Nat. Phys.* **11** 713
[28] Li S, Yan H, He Y and Wang H 2018 *Phys. Rev. A* **98** 022334
[29] Ye Q Z, Liang Z T, Zhang W X, Pan D J, Xue Z Y and Yan H 2022 *Phys. Rev. A* **106** 012407
[30] Ulanov A E, Sychev D, Pushkina A A, Fedorov I A and Lvovsky A I 2017 *Phys. Rev. Lett.* **118** 160501
[31] Van Loock P, Ladd T, Sanaka K, Yamaguchi F, Nemoto K, Munro W and Yamamoto Y 2006 *Phys. Rev. Lett.* **96** 240501
[32] Zhao P, Zhong W, Du M M, Li X Y, Zhou L and Sheng Y B 2024 *Front. Phys.* **19** 51201
[33] Djordjevic I B 2022 *IEEE Access* **10** 23284
[34] Do H, Malaney R and Green J 2021 *Quant. Engin.* **3** e60
[35] Omkar S, Teo Y S and Jeong H 2020 *Phys. Rev. Lett.* **125** 060501
[36] Kurizki G, Bertet P, Kubo Y, Mølmer K, Petrosyan D, Rabl P and Schmiedmayer J 2015 *Proc. Natl. Acad. Sci. USA* **112** 3866
[37] Shukla C, Malpani P and Thapliyal K 2021 *Quantum Inf. Process.* **20** 1
[38] Yan P S, Zhou L, Zhong W and Sheng Y B 2023 *Sci. China Phys. Mech.* **66** 250301
[39] Bennett C H, Brassard G, Popescu S, Schumacher B, Smolin J A and Wootters W K 1996 *Phys. Rev. Lett.* **76** 722
[40] Zhou L, Zhang S S, Zhong W and Sheng Y B 2020 *Ann. Phys.* **412** 168042
[41] Hu X M, Huang C X, Sheng Y B, Zhou L, Liu B H, Guo Y, Zhang C, Xing W B, Huang Y F, Li C F and Guo G C 2021 *Phys. Rev. Lett.* **126** 010503
[42] Wang G Y, Li T, Ai Q, Alsaedi A, Hayat T and Deng F G 2018 *Phys. Rev. Appl.* **10** 054058
[43] Preti F, Calarco T, Torres J M and Bernád J Z 2022 *Phys. Rev. A* **106** 022422
[44] Riera-Sàbat F, Sekatski P, Pirker A and Dür W 2021 *Phys. Rev. Lett.* **127** 040502
[45] Parker S, Bose S and Plenio M B 2000 *Phys. Rev. A* **61** 032305
[46] Rebic S, Mancini S, Morigi G and Vitali D 2010 *J. Opt. Soc. Am. B* **27** A198
[47] Fiurášek J, Marek P, Filip R and Schnabel R 2007 *Phys. Rev. A* **75** 050302
[48] Jeong K and Lim Y 2016 *Phys. Lett. A* **380** 3607
[49] Yan P S, Zhou L, Zhong W and Sheng Y B 2022 *Front. Phys.* **17** 21501
[50] Pan J W, Gasparoni S, Ursin R, Weihs G and Zeilinger A 2003 *Nature* **423** 417
[51] Chen L K, Yong H L, Xu P, Yao X C, Xiang T, Li Z D, Liu C, Lu H, Liu N L, Li L et al. 2017 *Nat. Photonics* **11** 695
[52] Reichle R, Leibfried D, Knill E, Britton J, Blakestad R B, Jost J D, Langer C, Ozeri R, Seidelin S and Wineland D J 2006 *Nature* **443** 838
[53] Kalb N, Reiserer A A, Humphreys P C, Bakermans J J, Kamerling S J, Nickerson N H, Benjamin S C, Twitchen D J, Markham M and Hanson R 2017 *Science* **356** 928
[54] Yan H, Zhong Y, Chang H S, Bienfait A, Chou M H, Conner C R, Dumur É, Grebel J, Povey R G and Cleland A N 2022 *Phys. Rev. Lett.* **128** 080504
[55] Sheng Y B, Zhou L and Long G L 2013 *Phys. Rev. A* **88** 022302
[56] Luo C C, Zhou L, Zhong W and Sheng Y B 2022 *Quantum Inf. Process.* **21** 300
[57] Luo C C, Zhou L, Zhong W, Du M M, Li X Y and Sheng Y B 2024 *Ann. Phys. (Berlin)* **536** 2300494
[58] Liu Y T, Wu Y M and Du F F 2022 *Chin. Phys. B* **31** 050303
[59] Du F F, Fan G, Wu Y M and Ren B C 2023 *Chin. Phys. B* **32** 060304
[60] Das S, Paul G, Banerji A 2020 *Phys. Rev. A* **102** 052401
[61] Yan P S, Zhou L, Zhong W and Sheng Y B 2022 *Phys. Rev. A* **105** 062418
[62] Zwerger M, Briegel H and Dür W 2013 *Phys. Rev. Lett.* **110** 260503
[63] Wallnöfer J and Dür W 2017 *Phys. Rev. A* **95** 012303
[64] Yan P S, Zhou L, Zhong W and Sheng Y B 2021 *Opt. Express* **29** 9363
[65] Wang P, Zhang Z, Yu C Q, Yuan R Y, Du F F and Ren B C 2023 *Ann. Phys.* **535** 2200505
[66] van Loock P, Lütkenhaus N, Munro W J and Nemoto K 2008 *Phys. Rev. A* **78** 062319
[67] Zeilinger A, Horne M A, Weinfurter H and Żukowski M 1997 *Phys. Rev. Lett.* **78** 3031
[68] Zheng C H, Zhao J, Shi P, Li W D and Gu Y J 2014 *Opt. Commun.* **316** 26
[69] Jeong H and An N B 2006 *Phys. Rev. A* **74** 022104